Eating Pathogens: A study of macrophage phagocytosis and the effects of the extracellular matrix

Alan Egan

Submitted for the degree of Master of Philosophy

Heriot-Watt University

Institute of Biological Chemistry, Biophysics and Bioengineering

July 2017

Abstract

Macrophages derive from multipotent precursor cells and play a critical role in the immune response. They can change states in response to environmental factors and much of these have been elucidated from a molecular biological approach. However, recent studies demonstrate that the biomechanical properties of the extra cellular matrix (ECM), such as stiffness, can affect the activation state of macrophages and possibly their ability to phagocytose. Phagocytosis, where a cell internalises a foreign object, by macrophages is a first line of defence against foreign bodies and is initiated by a receptor-ligand interaction which causes the polymerisation of actin to form the phagocytic cup which then goes on to become a phagosome. In this study, RAW264.7 and bone marrow derived macrophage (BMDM) cells were exposed to lipopolysaccharides (LPS) fluorescent bioparticles and zymosan fluorescent beads to study the phagocytosis process. The cells were investigated using time-lapse imaging and super-resolution microscopy. To understand the effects of ECM stiffness on phagocytosis, the cells were cultured on soft and stiff Polydimethylsiloxane (PDMS) elastomers to establish if substrate stiffness influences the phagocytic process. These results demonstrated that PDMS is not a good substrate for cell culture stiffness experiments. Using PDMS alone does not allow cells to adhere correctly and utilising ECM proteins as an adherence layer is also not feasible for stiffness studies as it negates the stiffness of the underlying substrate at the nanometre level. The live-imaging studies also revealed a possible new mechanism of phagosome formation.

Project Aims

To study the effect that the elastic modulus of substrates has on macrophages, specifically on their ability to phagocytose. This may correlate to how macrophages react to tissue stiffness in tumours or scar tissues.

Using live cell imaging and super resolution microscopy, the phagocytic process will be studied with particular focus on the phagocytic cup and phagosome formation. Many proteins are known to be involved in this process and more have been implicated. This study will look at some of these proteins with what looks to be the first time using super-resolution microscopy. Structured illumination microscopy will be utilised to do this in order to visualise protein localisation in the macrophage cell lines.

ACADEMIC REGISTRY
Research Thesis Submission

Name*:*	Alan Egan		
School:	Institute of Biological Chemistry, Biophysics and Bioengineering		
Version: *(i.e. First, Resubmission, Final)*	Final	Degree Sought:	Master of Philosophy

Declaration

In accordance with the appropriate regulations I hereby submit my thesis and I declare that:

1) the thesis embodies the results of my own work and has been composed by myself
2) where appropriate, I have made acknowledgement of the work of others and have made reference to work carried out in collaboration with other persons
3) the thesis is the correct version of the thesis for submission and is the same version as any electronic versions submitted*.
4) my thesis for the award referred to, deposited in the Heriot-Watt University Library, should be made available for loan or photocopying and be available via the Institutional Repository, subject to such conditions as the Librarian may require
5) I understand that as a student of the University I am required to abide by the Regulations of the University and to conform to its discipline.
6) I confirm that the thesis has been verified against plagiarism via an approved plagiarism detection application e.g. Turnitin.

* *Please note that it is the responsibility of the candidate to ensure that the correct version of the thesis is submitted.*

Signature of Candidate*:*		Date:	

Submission

Submitted By *(name in capitals):*	
Signature of Individual Submitting:	
Date Submitted:	

For Completion in the Student Service Centre (SSC)

Received in the SSC by *(name in capitals):*			
Method of Submission *(Handed in to SSC; posted through internal/external mail):*			
*E-thesis Submitted (**mandatory for final theses)***			
Signature:		Date:	

TABLE OF CONTENTS

Chapter 1 - Literature Review

1.1 Macrophages

Macrophages are the "Big Eaters" of the innate immune system, ubiquitous, functionally diverse cells first described by Metchnikoff in 1892[1][2]. They are phagocytic cells which are mainly involved in homeostasis by removing apoptotic cells, clearing of cellular debris, the remodelling of tissue after insult and most notably, defence against microbes[3].

The location of the macrophage populations gives rise to different phenotypes and they have been named due to the tissues they reside in. Macrophages resident in the liver are known as Kupffer cells, microglia are resident in the brain, Langerhans cells are found in the epithelium to name a few. In table 1.1, the location of these tissue resident macrophages can be seen along with the specialised functions they utilise in these locations.

Name	Function
Macrophage (Eye)	Vascular remodelling
Alveolar Macrophage (Lungs)	Immune surveillance
Kupffer Cells (Liver)	Debris clearance from blood and liver regeneration
Crypt Macrophages (Intestines)	Immune surveillance
Macrophage(Ovaries)	Ovulation and hormone production
Macrophage (Testis)	Hormone production
Osteoclasts (Bone)	Bone remodelling
Microglia (Brain)	Debris and dead cell clearance
Langerhans Cells (Skin)	Immune surveillance and keratinocyte differentiation
Macrophage (Cardiac)	Healing and remodelling
Macrophage (Kidney)	Ductal development
Bone Marrow Macrophage	Erythropoiesis
Macrophage (Mammary)	Ductal development and branching
Macrophage (Spleen)	Immune surveillance

Table 1.1 Macrophage phenotype and Function*[4]*

Traditionally, the ontology of macrophages was thought to arise from bone marrow monocytes differentiating in tissues to become tissue resident macrophages[5]–[7]. Although bone marrow monocytes move from the blood and enter tissues differentiating into macrophages during times of inflammation, recent research has shown that populations of tissue resident macrophages are derived from embryonic progenitors that are recruited to tissues during foetal development. These macrophages persist and account for a large amount of tissue-resident macrophages in adults[8], [9]. The ontology can be seen below in Figure 1.1.

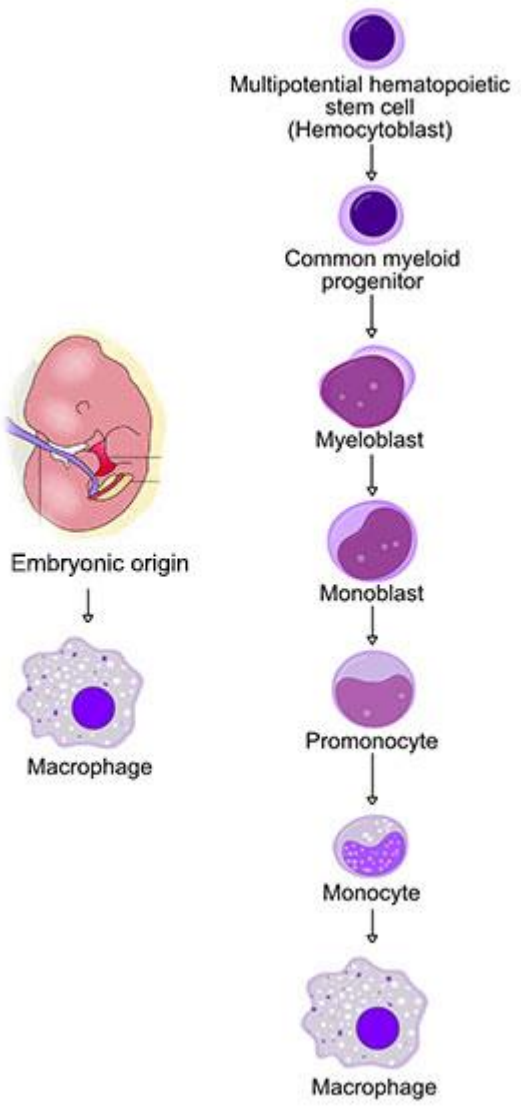

Figure 1.1 illustrates the lineage of macrophages from their multipotent precursor cells to monocytes and finally into macrophages and also from their embryonic origin. (Modified image from Copyright © [2006] [A. Rad])

1.2 Activation States

Macrophages can have different activation states which can change depending on environmental conditions. There are broadly two distinctive phenotypes, classically activated or M1 type and alternatively activated or M2 type which are extremes of a wide range of functional states[10][11]. Another phenotype of macrophage activation is present in tumour tissues, these macrophages represent a major factor in the inflammatory microenvironment of cancer and are referred to as Tumour associated macrophages (TAMs)[12].

These activation states can depend on the location of the macrophage in the body as certain phenotypes arise from adaption to their location such as microglia in the brain or Kupffer cells in the liver. These phenotypes are advantageous as different tissues require altered potencies of defence. Intestinal macrophages lining the gut for example do not need to initiate a chronic immune response that can be detrimental to health[13]. M1 and M2 macrophages have been shown to be capable of changing their activation state when exposed to different stimulus[14]. This further shows the plasticity of these adaptable cells and utilising this ability may be a way to provide a therapeutic effect in some auto-immune conditions and also possibly to re-programme TAMs to attack cancer cells.

1.2.1 M1 Phenotype Macrophage

M1 phenotype macrophages are known for their phagocytic ability. They are able to phagocytose a large numbers of units, be it cellular debris or pathogens. A number of stimuli can polarise macrophages to an M1 phenotype, the main three being lipopolysaccharide (LPS), Interferon-gamma (IFN- γ) and granulocyte-macrophage colony stimulating factor (GM-CSF). These activated cells can detect pathogens through receptors on the cell surface by direct pattern recognition receptors (PRRs) or by indirect receptors such as Fc or complement and when the cells become activated they have been shown to increase the number or receptors available on the cell surface[15].

As well as their phagocytic ability, M1 type macrophages produce pro-inflammatory cytokines such as tumour necrosis factor (TNF), IL-12, and IL-1β. An increase in reactive oxygen species (ROS) and inducible nitric oxide synthase (iNOS) production are also features of an M1 phenotype[16].

1.2.2 M2 Phenotype Macrophage

While M1 type macrophages are involved in destroying and removing pathogens, M2 type macrophages are anti-inflammatory and promote tissue repair and cell proliferation by arginine[17][18]. Some of the stimuli responsible for M2 activation are IL-4, IL-10, TGF-β as well as parasitic worms[19]. They have many different roles including, allergy response, angiogenesis and tissue remodelling to name a few[16]. The M2 type macrophage is further split into three classes, all having similar phenotype but with different functions. The M2a type are involved with the Th2 immune response and are known for their response to fungal or parasitic infections. The M2b type play a role in immune regulation and M2c macrophages are heavily involved in tissue remodelling[20].

1.2.3 Tumour-Associated Macrophages

For a cancerous tumour to have progressed, it must have found a way to supress the immune system. Macrophages found in the tumour microenvironment are known as tumour associate macrophages (TAMs). These are an M2 like class of macrophages and contribute to immune suppression. They do this by production of TGF- β and IL-10 which affect T-cells[21]. TAMs have been shown to be involved in metastasis, angiogenesis, tumour cell proliferation and lead to a poor prognosis[22]. As mentioned above, the plasticity of macrophages and the fact that they are not terminally differentiated into a particular activation state would suggest that reprogramming TAMs to an M1 type like state could possibly be a way of fighting cancer.

1.3 Phagocytosis

Phagocytosis has long been known as a main role of macrophages where they provide a first line of defence against foreign bodies as well as the clearing up of apoptotic, senescent, or dying cells. It is the engulfment of particles greater that 500 nm in size into a membrane-bound vesicle in the cytoplasm of cells. Macrophages are particularly known for their phagocytosis ability which they utilise in pathogen defence and apoptotic cell clearance. The initiation of phagocytosis begins when receptors on the macrophage sense ligands on a pathogen or cellular debris. The receptor ligand interaction causes the membrane to remodel and cup formation to begin. Pseudopods emerge from the cell membrane and reach for the target and eventually wrap around it, pulling it into the phagocytic cup. The cup then closes over the object to form a membrane bound vesicle called a phagosome. The phagosome then is met with lysosomes and endosomes to mature into a phagolysosome. The phagolysosome is an acidic environment similar to lysosomes and also contains other microbiocidal components such as hydrolyases, peroxidases and proteases, all of which help with pathogen degradation. Once the pathogen has been digested the macrophage expels the debris and begins antigen presentation to recruit and activate other immune cells. Figure 1.2 shows the stages of phagocytosis.

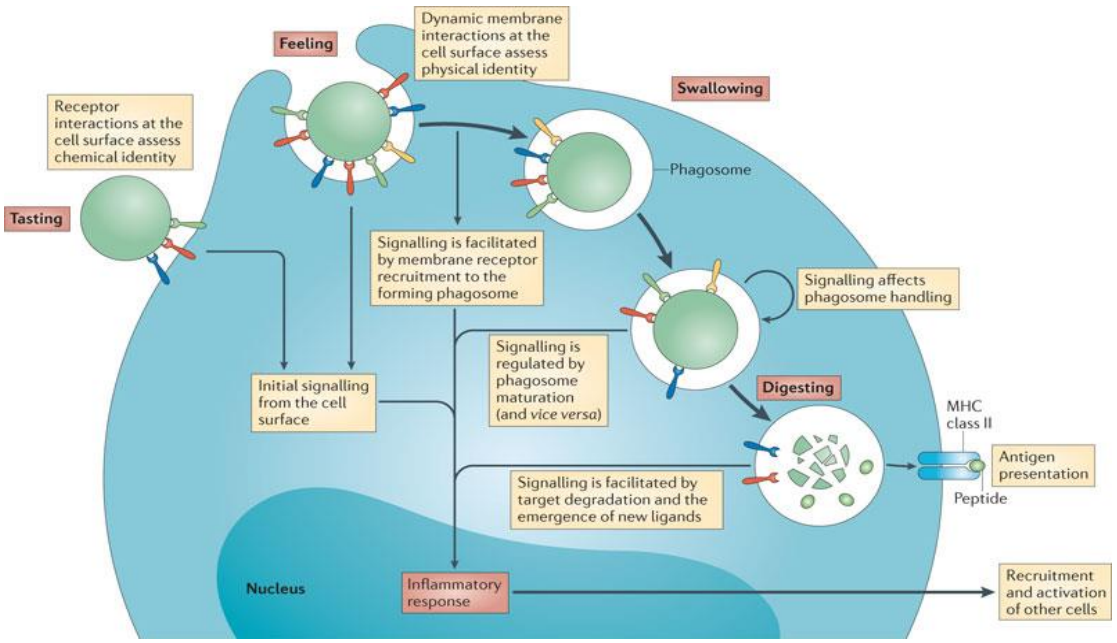

Figure 1.2 The stages involved in phagocytosis. Receptor interactions trigger the formation of the phagocytic cup to engulf the particle to form a phagosome. Underhill and Goodridge (2012)

Phagocytosis can be initiated in different ways depending on the pathway. Figure 1.3 illustrates the most common 2 types, Fc receptor mediated and complement receptor mediated phagocytosis.

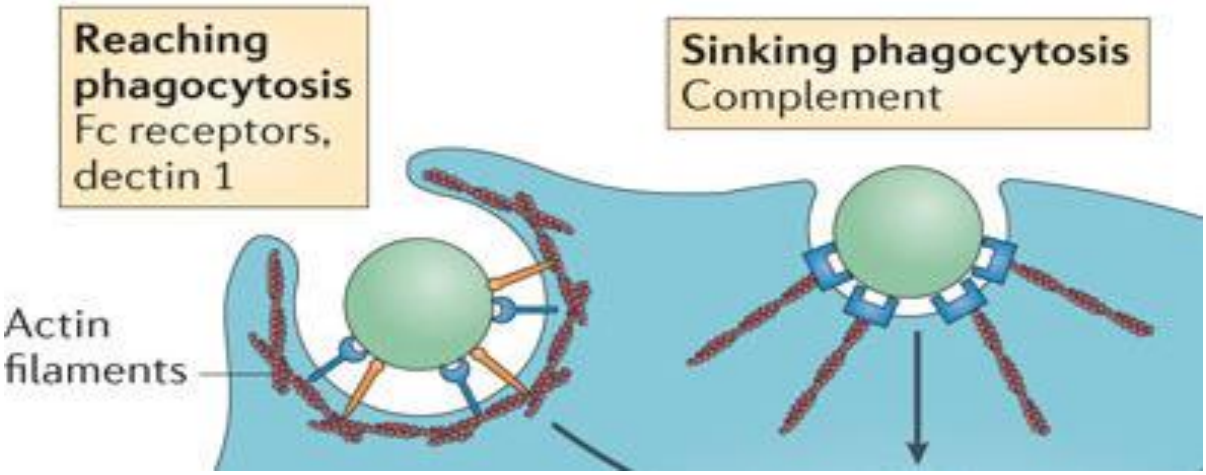

Figure 1.3 Illustrates Fc receptor mediated and Complement receptor mediated phagocytosis. Underhill and Goodridge (2012)

There are other receptors responsible for phagocytosis initiation including, scavenger receptors, MARCO, CD14, CD36 and dectin-1 receptors.

1.4 Lipopolysaccharides

Lipopolysaccharides (LPS) are a main component of the outer membrane of gram-negative bacteria. They act as a defensive barrier whereby they provide the cell with protection from environmental stress, even allowing some bacteria to survive in extreme environments[23]. LPS has long been used in immune studies as it is a very strong stimulator of the innate immune response in eukaryotes and in high quantities it can cause the host to go in to septic shock.

LPS is composed of three parts; an O-antigen, a carbohydrate core and a Lipid A. It is the Lipid A unit that causes the strong immune response due to its activation of the pattern recognition receptor (PRR) Toll Like Receptor 4 (TLR4). Lipid A is not normally accessible until the bacterial cell replicates or due to other mechanisms that lead to parts of the cell wall to separate. This allows the Lipid A unit to become extracellular and to be picked up by the innate immune system leading to the TLR4 pathway of immune response[24].

1.5 Zymosan

Like LPS, zymosan has been utilised in immune response studies for many decades now. It is recovered from the cell wall of a yeast, namely *Saccharomyces cerevisiae*. It is also a strong stimulator of the innate immune response, but its mechanism of action is different to that of LPS. The phagocytosis of zymosan is facilitated by a range of receptors, most notably the mannose receptor (MR). Conversely, the immune response initiated by zymosan is dependent on single a receptor which is a heterodimer of TLR2 and TLR6. Interestingly, Underhill *et al.* demonstrated that both the phagocytosis and immune response are not inter-reliant and one can take place regardless of the other[25].

1.6 Substrate Influence on Macrophages

The substrates on which cells are cultured been known to affect cell behaviour for a long time. Many studies have been done showing how stem cells can be differentiated as a result of the properties of the substrate they adhere to[26]–[28]. This can be down to a number of factors including, stiffness, topography, adhesivity, hydrophobicity, chemical composition and binding affinity. Adherent cells have many integrins which interact with substrate ligands to provide traction for the cell. The strength of this traction lead to forces in the cell which can affect cell morphology and cytoskeletal arrangement. This in turn can affect cell function and even gene expression. Kilian and Mrksich showed using RT-PCR that lineage specific gene expression varied across four different substrates[27]. Engler et al. also demonstrated that mesenchymal stem cells commit to lineages as dictated by the elasticity of the substrate they were cultured on[28].

It has been reported that the biomechanical properties of the ECM can affect the activation state of macrophages[29]. Most of these studies have used ECM proteins on their substrates and not taken this into account when measuring the elastic modulus of the substrates. The stiffness testing that has been done was by tensile tests where they stretched the substrates in order to calculate the stiffness or by compression tests[30] on a large area of the substrate. These methods completely ignore the effect of the topical ECM proteins and other studies measure the substrates stiffness before coating with an ECM protein[31][32]. The affect ECM proteins have on the substrate stiffness does not seem to be taken into account in these studies which would question the role stiffness has to play in their results.

1.7 Proteins Involved in Phagocytosis

Many proteins are known to be involved in the phagocytic process and many others have been implicated. The proteins of interest for this project are Rac1, RhoA, PTEN, vinculin, paxillin, and talin.

1.7.1 Rho GTPase family

The Rho GTPase family are heavily involved in the control of actin reorganisation which is critical for phagocytosis. The signalling pathways involved in this process are not fully elucidated, but once a receptor ligand interaction has been made, actin polymerization beneath the site begins. This actin polymerisation leads to the formation of the phagocytic cup and pseudopodia extensions. The Rho GTPases are responsible for actin filament organisation which control the motility and phagocytosis process of engulfment. The most common proteins of the Rho GTPase family involved in the process are Rac1, RhoA and Cdc42.

1.7.2 PTEN

Phosphatase and tensin homolog (PTEN) is a ubiquitous phosphatase. It is a tumour suppressor and its main role is to dephosphorylate PIP3 to form PIP2 which results in inhibition of the AKT signalling pathway. Mondal *et al*. demonstrated that depletion of PTEN in macrophages resulted in an increased PIP3 expression which led to enhanced phagocytosis *in vitro* and *in vivo*[33]. Kim *et al*. also showed that wildtype PTEN completely disabled Fc mediated phagocytosis in Cos 7 cells[34].

1.7.3 Vinculin

Vinculin is a protein involved in integrin adhesion to the actin cytoskeleton. It is heavily involved in cell-substrate interaction as well as cell to cell interactions. It has been shown to be involved in the phagocytic cup formation[35]. Hagiwara *et al.* demonstrated that vinculin is involved in phagocytosis where by it binds to *Staphylococcus aureus* and leads to its engulfment[36].

1.7.4 Paxillin

Like vinculin, paxillin is a protein involved in the adherence of cells to the ECM. It binds to vinculin in focal contacts. Gitik *et al.* showed that phagocytic receptors activate phagocytosis though paxillin[37]. It has also been shown that in Fc mediated phagocytosis, paxillin phosphorylation increases and its distribution changes from the cytoplasm to the cytoskeleton depending on the different phases of phagocytosis[38].

1.7.5 Talin

Another cytoskeleton protein involved in cell adherence and cell to cell contact is talin. Talin also binds to vinculin where it stabilises the cell to substrate junctions by linking the integrins to the acting cytoskeleton. As the proteins involved in cell adhesion are also the proteins mostly involved in phagocytosis, talin had an important role to play in phagocytosis. Previous studies have shown that talin is involved in phagosome forming in Fc and complement mediated phagocytosis and that its knockdown specifically reduces complement mediated phagocytosis[39]. In Fc mediated phagocytosis, talin co-localises with actin where it gathers next to the phagocytic cup. As well as that, is also found in the pseudopodia that begin to engulf and draw the pathogen into the cell membrane in which actin is also heavily involved[40].

1.8 Super-Resolution Microscopy

Microscopy is the study of objects that cannot be seen by the naked eye. There are many factors which can affect the resolution of an optical microscope such as, quality of lenses and the alignment of said lenses. Even if the lens was 100% perfect in quality and alignment, the microscope resolution is still only as good as its diffraction limit. In 1873, Abbe discovered that the resolution of an optical system depended on the wavelength of light, the refractive index of the material and the maximum angle against the axis which can still get into the objective of the lens being used. Using these he came up with an equation to calculate the theoretically possible resolution of a microscope.

$$d = \frac{\lambda}{2n\sin\theta}$$

Where d is the resolution of the microscope, λ is the wavelength of light and $n\sin\theta$ is the numerical aperture of the lens being used. Green light has a wavelength of around 500 nm, if it was imaged with an objective with an NA of 1 for example, it would give a lateral resolution of around 250 nm. This seems like a very small size but 250 nm is relatively large for the biological study of proteins which require much smaller resolutions to be able to image their localisation correctly. For this reason, super-resolution microscopy will be will be utilised in this study.

Over the last couple of decades there have been significant developments in "breaking" the diffraction limit of light to increase the resolving power of microscopes. The point spread function (PSF) as seen in figure 1.4 is a result of the diffraction of light. It blurs the light source image creating an Airy disk which makes it difficult to see the actual size of the light source and even to differentiate if it is one single point source or many.

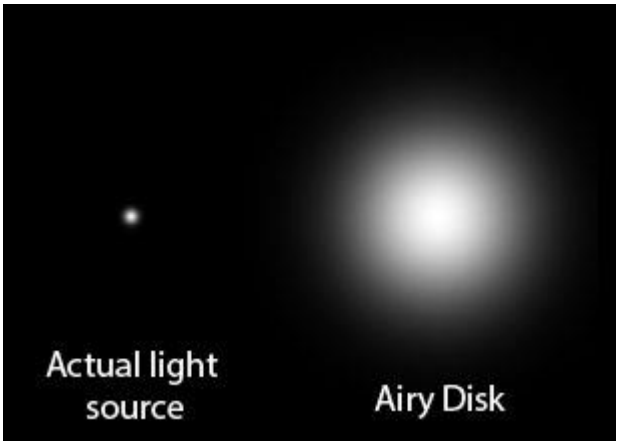

Figure 1.4 A simulated image of the PSF showing the actual pinpoint light source on the left and the resulting image as seen through the microscope objective due to the diffraction limit of light.

Today there are many instruments and techniques for overcoming the diffraction limit of light and it is now possible to successfully achieve lateral resolutions of around 10 nm which makes super-resolution ideal for looking at the proteins involved in the phagocytosis process.

1.8.1 Structured Illumination Microscopy

Structured Illumination microscopy (SIM) is a fluorescence imaging technique that uses moiré patterns to construct a Fourier transform containing more frequencies than would be normally available. It does this by shining different patterns of light on the sample in order to create a *moirés* effect. The frequency domain is then reconstructed into a super-resolution image. Advances in this technique can get down to resolutions of about 50 nm both laterally[41]. As well as that, sample preparation is the same as it is for widefield fluorescence microscopy. The major drawback with SIM is the length of time it takes to capture the images and to reconstruct them afterwards. For this reason, it is more suited to fixed cell imaging. Figure 1.5 shows a comparison of a widefield image compared to a SIM image.

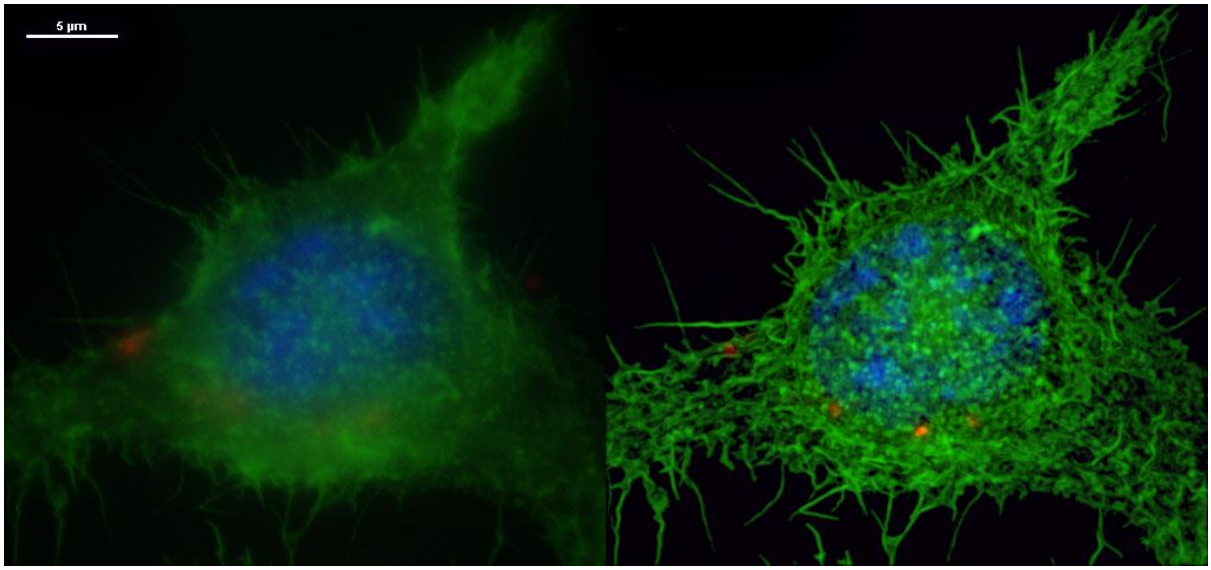

Figure 1.5 Raw264.7 cells with pHrodo LPS bioparticles (red), actin in green (phalloidin) and the cell nucleus in blue (DAPI). The widefield image is on the left and the SIM image is on the right is much superior in its resolution.

1.8.2 Stimulated Emission Depletion Microscopy

Another method of overcoming the diffraction limit is with the use of stimulated emission depletion (STED) microscopy. This technique uses a high power laser in a ring shape around the excitation laser in order to bleach all other fluorophores except the one of interest inside the ring which can be excited as normal with the excitation laser. The ring power can be increased or decreased to allow minimising of the illumination at the point of interest which increases the resolution[42]. Stefan Hell won the 2014 Nobel Prize in chemistry for the development of this technique. Advances in this method have been shown to achieve resolutions down to 2.1 nm[43].

1.8.3 Single Molecule Localisation Techniques

There are many other techniques based on single molecule localisation methods such as stochastic optical reconstruction microscopy (STORM)[44] and photoactivated localisation microscopy (PALM)[45]. Both of these are widefield techniques and work by stochastically activating fluorophores through multiple cycles and rapidly capturing many images which can be reconstructed to show each fluorophore as it was activated. This allows the software to assume that each source of light was from one fluorophore only which creates a super-resolution image. This method can get to 10 nm lateral resolution[46].

Chapter 2 - Methods

The project required two cell lines and one primary cells to be cultured and maintained. For imaging, staining needs to be optimised, and substrates of choice need to be prepared to grow and image cells on them. The substrate stiffness also needs be measured.

2.1 Raw 264.7 cell line

These are a macrophage-like cell line derived from Balb/c mice. They preserve many of the properties of macrophages such as phagocytosis of beads and Zymosan, high nitric oxide (NO) production, are very responsive to TLR agonists and they also possess suitable motility for study. They are capable of being transfected. The cell line was received from Dr Fiona Semple at the Institute of Genetic and Molecular Medicine, Edinburgh. The cells were cultured in T75 flasks with Dulbecco's Modified Eagle Medium (DMEM) supplemented with 10% heat inactivated foetal bovine serum (HI-FBS) and pen/strep. This model has been one of the main cell lines utilised for macrophage studies for many years.

2.2 Passaging cells

When cultures were 70-80% confluent they were passaged as follows. Spent culture medium was discarded and the cell layer was washed with DPBS. Fresh media was added and cells were scraped to remove them from the flask substrate. Appropriate aliquots were taken (usually a 1:4 to 1:6) and resuspended in fresh media in a new culture vessel and placed in an incubator at 37 °C with 5% CO_2.

2.3 Cell fixation and immunofluorescence staining

Media and reagents were warmed to room temperature and spent culture medium was aspirated and discarded. Cells were grown on square 22mm glass coverslips, each one placed in a well of a 6-well plate. The coverslips were firstly washed with DPBS and then incubated for 20 mins with 4% Polyformaldehyde (PFA) to fix the cells. The coverslips were then washed in triplicate with DPBS to remove any PFA. They were then incubated for 5 mins with 0.2% Triton X-100 in order to permeablize the cells, once permeabilized they were again washed in triplicate with DPBS. If antibodies were being used, the coverslips were incubated in a blocking buffer for 10 mins to stop unspecific binding, before being washed in triplicate with DPBS.

100 µl of primary antibodies were then added and incubate for 1-24 h depending on supplier recommended instructions and incubate at 4 ^{O}C. They were then washed in triplicate with DPBS before addition of 100 µl of secondary antibodies and left to incubate for 20 mins (DAPI and phalloidin can be also added at this stage if required). Finally, they were washed in triplicate with DPBS and mounted to microscope slide using 10 µl of mowiol cell side down and allowed to dry. The coverslips were then sealed with varnish and allowed to dry before imaging.

2.4 Resuscitating Cells

Media was warmed to 37 ^{o}C using a water bath. A frozen cell vial was removed from storage and the contents were thawed quickly in the 37 ^{o}C water bath. Using aseptic technique in a biological hood, the cells were pipetted into 10 ml of preheated media in an appropriate tube for centrifugation and spun at 80 g for 2 mins. Supernatant was aspirated to remove DMSO and the pellet was re-suspended in 10 ml of warmed media. A viable cell count was done using a Becton Dickson cell counter and cells were transferred to a correctly labelled T75 flask with date, initials, cell line and passage number. It was then placed in an incubator set to 37 ^{o}C and 5% CO_2 conc. Cells were then monitored daily and split when 70-80% confluent.

2.5 Freezing Cells

When cultures were 70-80% confluent they were frozen down as follows. Spent culture medium was removed and put aside to make freezing media. The cell layer was washed with DPBS and fresh media was added. The cells were gently scraped to remove them from the flask substrate and then transferred to a 15 ml falcon tube. A cell count was performed using a Becton Dickson cell counter. Cells were then spun down. Freeze media was made by combining 45% cell conditioned media with 45% fresh media and adding 10% DMSO. When the cells were spun down, media was removed, and the pellet was resuspended in freeze media to give a cell concentration of 5 x 10^6 cells/ml. 1 ml was then added to cryovials and placed in a *Mr. Frosty* which causes cells to be frozen slowly at 1 °C /min when placed in a -80 °C freezer. After 24 hr, they were then transferred to liquid nitrogen storage.

2.6 PDMS substrates

Sylgard 184 PDMS ratios of 5:1, 10:1 and 20:1 elastomer to curing agent mix were chosen to show a range of substrate stiffnesses. The mixtures were stirred thoroughly before being degassed to remove any air bubbles out of the mixture in a vacuum degasser. They were then poured into a 35 mm petri dish to a thickness of ~3mm and once again degassed. Once all bubbles had been removed, they were cured in an oven at 65 °C for 1 hour. Following curing, the plate was oxygen plasma treated using a *Diener* Electronic surface plasma system. The substrates were then covered with ethanol to prevent recovery before being cultured with cells.

2.7 Fixed Phagocytosis Assay

RAW264.7 cells were seeded at a concentration of 1.25 x 10^5 cells/well in a 6-well plate containing glass coverslips and placed in an incubator for 48 h at 37 ^oC and 5% CO_2. After 48 h, LPS Bioparticles or zymosan beads were added and it was placed back in the incubator for the desired time. The cells were then fixed and stained as above.

2.8 Live Phagocytosis Assay

Cells were seeded at a concentration of 1.25 x 10^5 cells/dish in a 35mm glass bottom dish and placed in an incubator for 48 h at 37 ^oC and 5% CO_2. After 48 h, the dish was taken to the microscope and placed in the incubation chamber on a *Nikon* A1R Laser Scanning Confocal Microscope. The time-lapse was initiated and LPS Bioparticles or zymosan beads were added.

2.9 Isolation of Murine Bone Marrow Derived Macrophages

Enteroendocrine L-cells were grown to confluence in DMEM with 10% HI-FBS with 100IU/ml penicillin and 100ug/ml streptomycin. The flasks were sealed and incubated for 3 weeks at 37^oC and 5% CO_2. The L-cell conditioned media was recovered and sterilised by filtration using a 0.25 um filter and stored at 4 ^oC. This media contains CSF-1 which is needed for bone marrow derived macrophage (BMDM) differentiation.

Femoral bone marrow cells were isolated from 50% C57BL6J and 50% FvB mice for Rac-1 FRET and 87.5% percent C57BL6J 3rd generation back cross from initial transgenic mouse for RhoA FRET. They were flushed with syringes from the bone using RPMI macrophage growth medium which contained 10% HI-FBS, 100 IU/ml penicillin, 100 µg/ml streptomycin, 1x non-essential amino acids, 1mM Sodium pyruvate and 8.5 µl of B-mercaptoethanol, supplemented with 10% L-cell conditioned media. Cells were seeded at 1 x 10^6 cells/ml in a 25 cm^2 bacterial plastic dish and incubated at 37 ^oC and 5% CO_2. After 3 days, non-adherent cells were collected and cryogenically frozen as above for later use as these cells have a limited proliferation life span.

2.10 Atomic Force Microscopy

AFM was carried out using an *JPK Nanowizard 3* Bioscience optimised for live cell imaging, mounted on a *Zeiss Axio Observer D1* Microscope completely contained in an acoustic enclosure. A Hertz contact model, a pyramidal gold coated tip with force constant of 0.3734N/m and angle of 35 degrees along with a set point of 5nN and a scan rate of 1Hz were utilised. The experiment was carried out three times on three separate days and >30 different contact points were measured for each sample.

Chapter 3 - Results and Discussion

The first step was to optimise the antibodies chosen for the project with the RAW264.7 cell line. The phagocytic assay was then developed and tested with fixed and live imaging followed by super-resolution microscopy of the fixed samples. The live imaging led to an investigation of phagocytic vesicles seen in the phagocytosis process that was not expected. Concurrently, a substrate was chosen and tested for substrate stiffness experiments with the cells.

3.1 Proteins of Interest

Three adhesion associated proteins were chosen for study; talin, vinculin and paxillin. The antibodies were optimised by using a 1/200th and a 1/500th dilution of the primary antibodies with representative images shown in figure 3.1 and table 3.1. Each experiment was done in triplicate and repeated on three separate days.

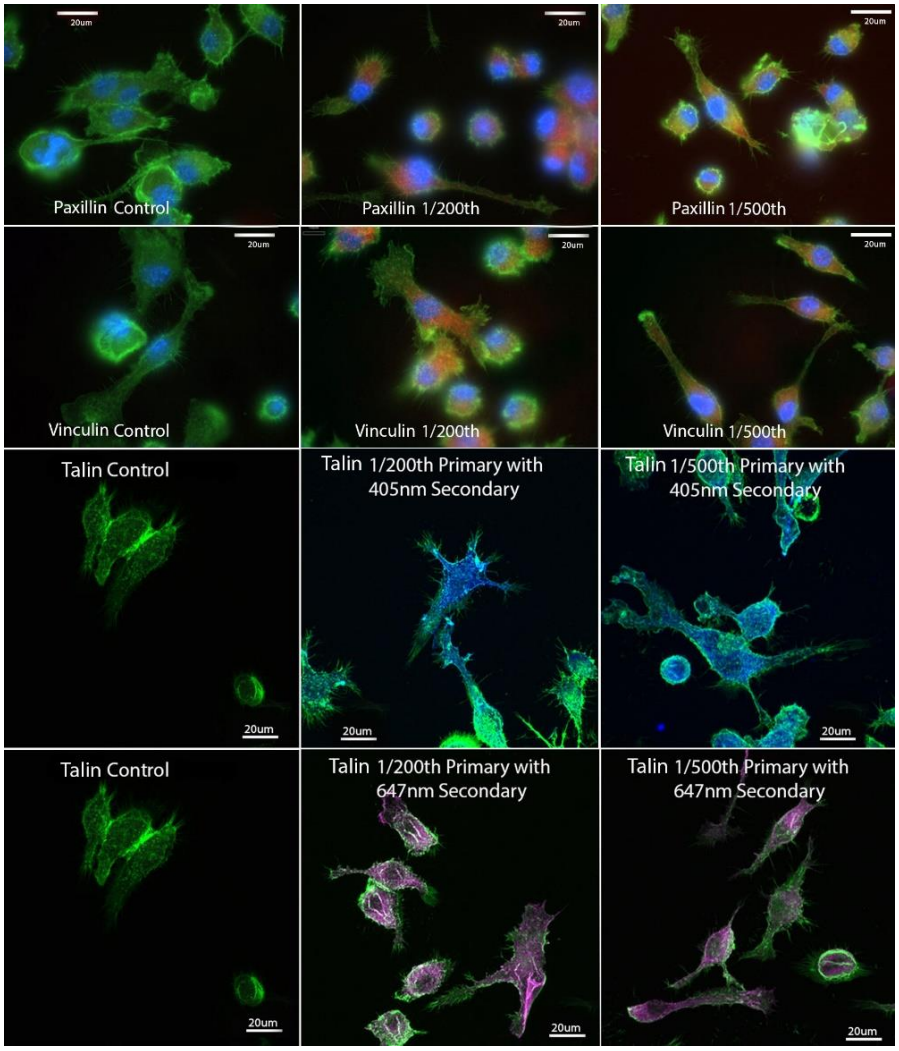

Figure 3.1 RAW264.7 cells were fixed and stained with paxillin, vinculin and Talin primary antibodies along with Alexa Fluor 405 (Blue) and Alexa Fluor 647 (Pink) secondary's for Talin, and Alexa Flour 568 secondary for paxillin and vinculin. Phalloidin (Green) was also used to stain for actin and DAPI (Blue) was used to stain the nucleus in vinculin and paxillin. Scale bar shown is 20 µm.

Antibody	1/200th Dilution	1/500th Dilution
Paxillin	Good	Weak
Vinculin	Good	Weak
Talin	Good	Good

Table 3.1 Antibody Optimisation. Optimal dilutions for each antibody highlighted in green.

3.1.1 Talin

The talin 1&2 (*abcam*) antibody staining worked successfully at 1/200th dilution and at 1/500th which mean 1/500th dilution will work for the planned experiments. Both of the secondary antibodies were successful which is very useful as it means we can stain at the 405 nm and also in the far red at 657 nm. As a result, we have the capability to perform four colour immunofluorescence staining which will be very beneficial as it will be possible to image actin in green with 488 nm and zymosan beads in red with 561 nm.

3.1.2 Vinculin

The Pierce vinculin antibody (*Novex*, 42H89L44) staining worked successfully for the primary and also for the 568 secondary antibody. The 1/500th dilution required a longer exposure time and more laser power which produced some noise in the image, therefore, a 1/200th dilution will be utilised for the experiments with this antibody.

3.1.3 Paxillin

The paxillin antibody (*Novex*, 5H11) staining worked successfully for the primary and also for the 568 secondary antibody. As with the vinculin antibody, the 1/500th dilution required a longer exposure time and more laser power which caused noise in the image, consequently, a 1/200th dilution will be employed for the experiments with this antibody.

Once the PDMS substrate adherence is addressed, these proteins will be studied on each of the substrates

3.2 Phagocytosis assay

Cells were seeded onto glass coverslips and after 48 h they were exposed to tagged Cy3 zymosan beads for 2h followed by fixing and staining by phalloidin for actin visualisation and DAPI for the nucleus. This was done to see if it was possible to visualise the different stages of the phagocytosis process using fixed imaging. These experiments were done in triplicate and repeated on three separate days.

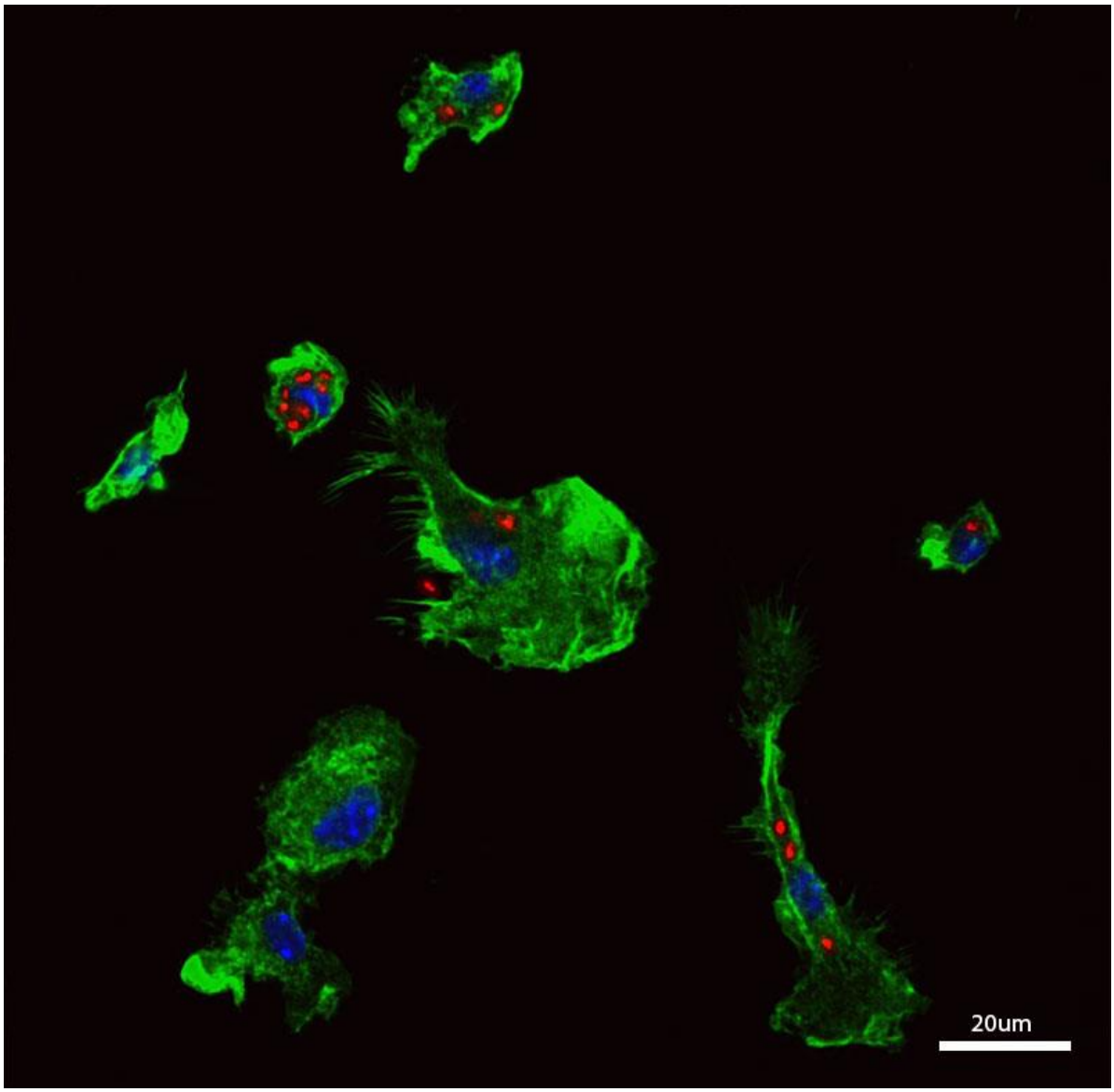

Figure 3.2 Raw264.7 cells showing phagocytosed cy3 tagged zymosan (red) after 1h incubation, actin in green (phalloidin) and the cell nucleus in blue (DAPI). Scale bar shown is 20 µm.

The Raw264.7 cells successfully phagocytosed the beads after a 2h incubation. This assay was successful and will allow a time point assay to be carried out by choosing times from the time-lapse images. Times will be chosen so cells can be fixed to capture the different stages of phagocytosis as some of the proteins of interest may not be involved in all stages of phagocytosis.

Time-lapse imaging of zymosan phagocytosis was carried out using the RAW264.7 cell line. Brightfield was used for the cells and a 561 nm laser was used for the zymosan beads. Figure 3.3 shows the phagocytosis process from cup formation to engulfment. Table 3.2 shows a breakdown of the number of cells that phagocytosed beads over a 2h period as well as how many beads were phagocytosed and how many cells did not phagocytose any beads. A total of 111 cells were analysed using ImageJ. The cells phagocytosed 96 beads over 2 hours and 55% of the cells had phagocytosed after a 2h period. This will be repeated on each of the substrates to see if substrate stiffness affects phagocytosis in macrophages.

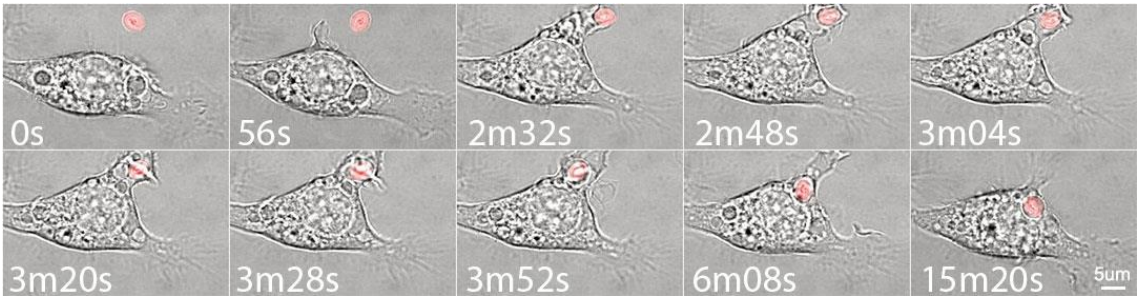

Figure 3.3 RAW264.7 cells showing phagocytosed cy3 tagged zymosan. These stills are taken from a time-lapse to show the phagocytosis process. Scale bar shown is 5 µm

	Number of Cells	Beads phagocytosed	Cells with no beads	Average Beads per cells	% cells that phagocytosed
Run 1	47	38	26	1.8	44.7
Run 2	32	32	12	1.6	62.5
Run 3	32	26	12	1.3	62.5
Total	111	96	50	1.6	55

Table 3.2 RAW264.7 cells showing phagocytosed cy3 tagged zymosan. These results are taken from a time-lapse to show the phagocytosis process over a 2h period.

Further data analysis optimisation of the time-lapse images was carried out using *imageJ* (Figure 3.4) to measure the morphological characteristics of the macrophages after exposure to the zymosan beads. Graph A shows the total surface area of the macrophages which has one peak to suggest not much variance in cell spreading between the cells. Graph B illustrates the roundness or circularity of the cells. Values of 1 demonstrate a circular morphology and values <1 suggest an irregular or elongated shape. Graph C shows the perimeter of the cells and this follows a similar pattern to the macrophage surface area with one main peak.

There are two strong peaks at ~0.45 and ~0.85 as well as a smaller peak at ~0.65 which suggest two populations of morphologies which isn't surprising as the cells can quickly go from a spherical shape to an elongated morphology depending on if they have phagocytosed or are reaching to interact with a bead and they have also been seen to do this regardless of any stimulus. This analysis can be carried out on the time-lapse images which will be done on the different stiffness substrates and all of the data compared.

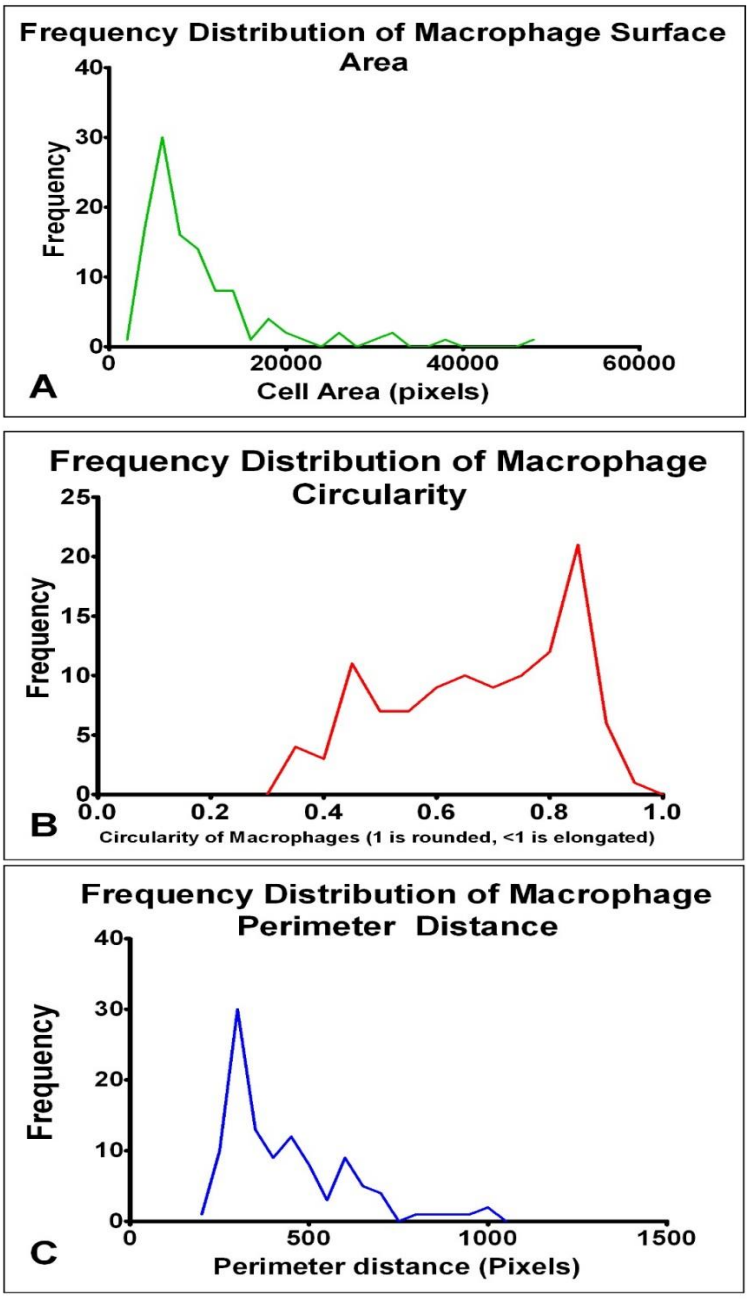

Figure 3.4 Graphs show the frequency distribution of the morphology of RAW264.7 cells after 2h exposure to zymosan beads. Graph A shows the total surface area of the macrophages which has one peak to suggest not much variance in cell spreading between the cells. Graph B illustrates the roundness or circularity of the cells. Values of 1 demonstrate a circular morphology and values <1 demonstrate an irregular or elongated shape. Graph C shows the perimeter or circumference of the cells and this follows a similar pattern to the macrophage surface area with one main peak (N=3).

3.3 Super-resolution Microscopy

The optimised vinculin antibody was also imaged using Super-resolution microscopy with the *Nikon* N-SIM microscope. It gave extremely well resolved images of vinculin showing its focal point of adherence to the substrate as seen in red in Figure 3.5. This will be repeated at different stages of the phagocytic process and also on the different stiffness substrates.

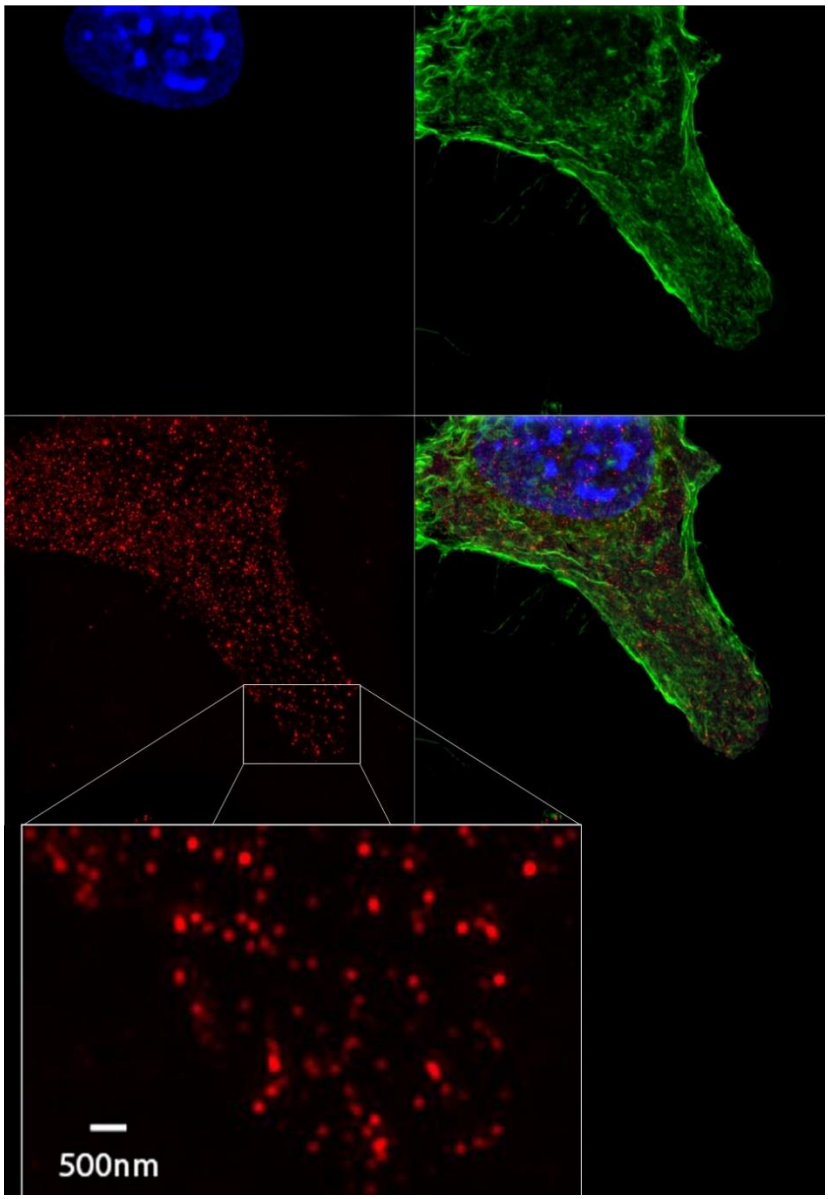

Figure 3.5 RAW264.7 cells were cultured on coverslips and incubated for 48 h before being fixed and stained with Vinculin primary antibody with a secondary Alexa flour 568 nm antibody. Phalloidin (Green) was also used to stain for actin and DAPI (Blue) to stain the nucleus.

Images of the LPS Bioparticles which had been endocytosed (not phagocytosed as less than 500 nm) were also optimised using the N-SIM instrument. These images can be seen in figure 3.6.

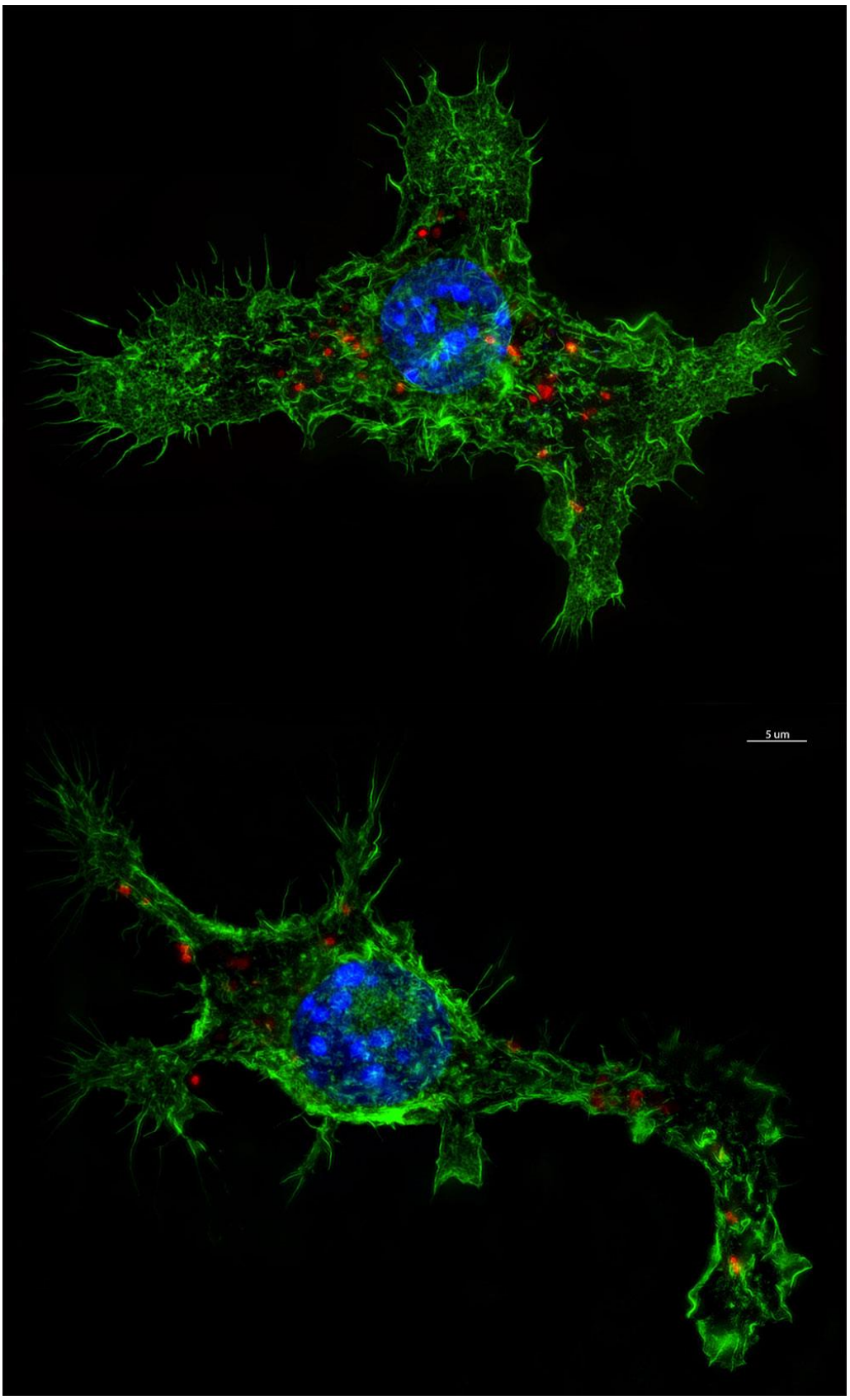

Figure 3.6 Raw264.7 cells showing endocytosed pHrodo LPS bioparticles (red) after 1h incubation, actin in green (phalloidin) and the cell nucleus in blue (DAPI). These images were taken as part of the optimisation of the SIM system for the cell line. Scale bar shown is 5 µm

3.4 Substrate Stiffness

Three ratios of PDMS were utilised for the experiment 5:1, 10:1 and 20:1 as they represent a range of stiffnesses. As macrophages are found all over the body, the stiffnesses they encounter are varied so no specific elastic moduli were chosen for this study. Previous studies have also used these ratios for cell experiments and found that a 10:1 ratio has the greatest elastic modulus. A 10:1 ratio is the manufacturer's recommended ratio and indicates this is the optimal concentration of cross linker. Ratios lower then 10:1 would have an excess of crosslinker which results in a lower elastic modulus in the 5:1 ratio[47, p. 2]. Conversely, the 20:1 ratio has less crosslinker available than the 10:1 and therefore also has a lower elastic modulus. The AFM results of the plasma treated substrates reflects this pattern. The 5:1 ratio measured 42 MPa, 10:1 measured 76 MPa and the 20:1 measured 58 MPa. These results fall within the range of expected values for plasma treated PDMS[48]. The plasma treatment causes a stiff layer to form on the PDMS which increases the elastic modulus of the substrate[48].

RAW264.7 macrophage cells were cultured directly onto the substrates and incubated to see if the cells would adhere to PDMS or if another option would be needed to help adherence. After 48 h the cells were fixed and stained with phalloidin and DAPI as above. Figure 3.7 shows the fluorescence imaging along with graphs of cell surface area, roundness and perimeter length. These experiments were done in triplicate and repeated on three separate days.

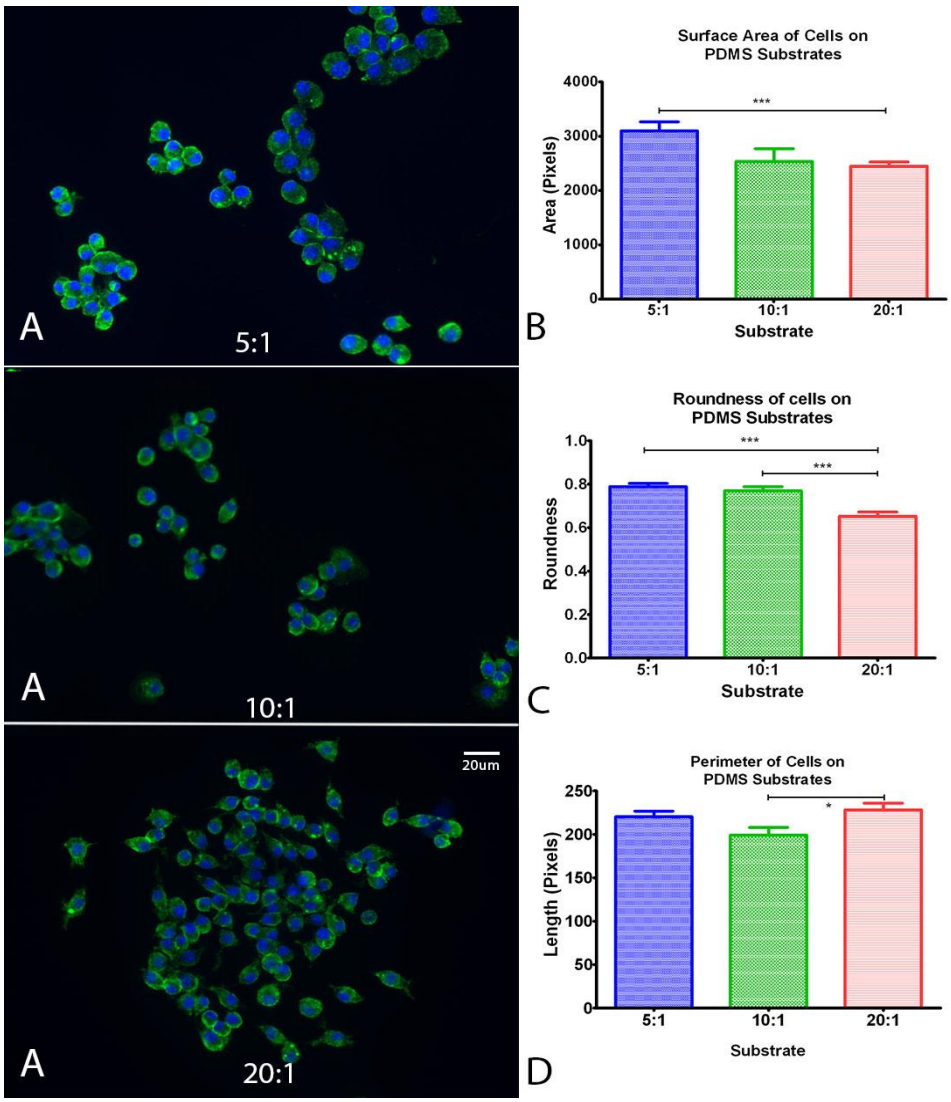

Figure 3.7 A. RAW264.7 Macrophages grown on 5:1, 10:1 and 20:1 PDMS substrates. After 48 h of incubation, cells were fixed and stained with actin in green (phalloidin) and the cell nucleus in blue (DAPI). B Average surface area of cells was measured and graphed. C Roundness of cells was calculated and graphed. D Perimeter of cells was measured and graphed for each substrate. Graphs show mean ± SEM (* -> P<0.001, ** -> P<0.01 and *->P<0.05) Scale bar shown is 20 µm (N=3).**

In comparison to culture on glass, the cells did not seem to adhere to the substrates very well with only sparse populations adhering throughout the substrate. The cells morphology was similar for 5:1 and 10:1 PDMS ratios with the 20:1 having a statistically significant greater spreading of cells as shown by their lower roundness value. The surface area of cells on the 5:1 substrate was significantly larger than the other two substrates, but the perimeter length was greater in the 20:1 substrate which suggests an elongated morphology. This was most likely down to the hydrophobicity of the PDMS substrates as the wettability of 5:1 and 10:1 was noticeably much less than that of the 20:1.

The next step was to find another way to treat the PDMS so the surface would be less hydrophobic and the cells would be more likely to adhere. Wang *et al*. oxidised the PDMS surfaces using oxygen plasma which reduces the hydrophobicity of the substrates[47]. This was carried out using a *Diener* Electronic surface plasma system. Treating the PDMS with oxygen plasma creates hydrophilic silanol groups (SiOH) but these hydrophilic functional groups are short lived in normal atmosphere as the substrate will recover back to its original hydrophobic nature[49]. Covering the treated substrate with ethanol or de-ionized water can help to prevent recovery.

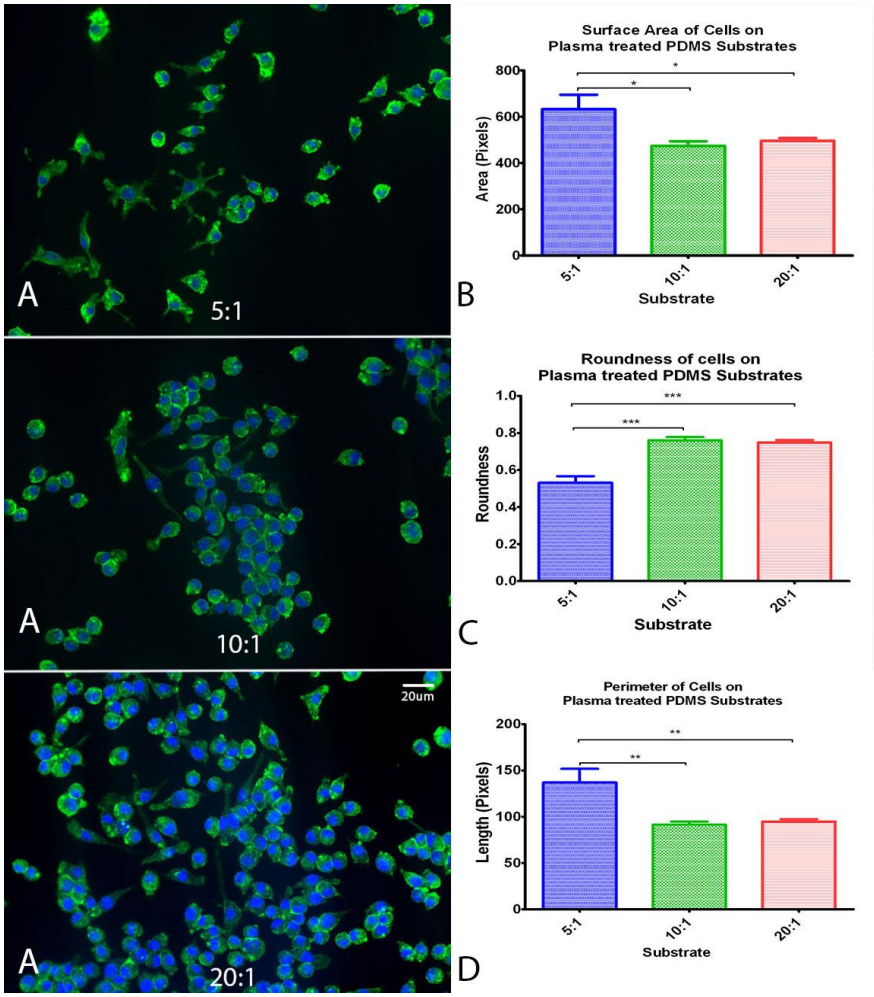

Figure 3.8 A. RAW264.7 Macrophages grown on 5:1, 10:1 and 20:1 plasma treated PDMS substrates. After 48 h of incubation, cells were fixed and stained with actin in green (phalloidin) and the cell nucleus in blue (DAPI). B Average surface area of cells was measured and graphed. C Roundness of cells was calculated and graphed. D Perimeter of cells was measured and graphed for each substrate. Graphs show mean ± SEM (* -> P<0.001, ** -> P<0.01 and *->P<0.05) Scale bar shown is 20 µm (N=3).**

After plasma treating the PDMS substrates, the cells adhered much better than they did on non-plasma treated PDMS. From the images and graphs in figure 3.8, the cells cultured on the plasma treated PDMS substrates had a morphology comparable to how they look cultured on glass, having a greater surface area, a more elongated shape and also a larger perimeter, suggesting better cell adherence and spreading.

The results from each of the morphology studies on PDMS and Plasma treated PDMS are compared and seen in figure 3.9. The morphology of the cells on the 5:1 substrate, which seems to be the more hydrophobic of the substrates changed when the surface was plasma treated. The cells were significantly more elongated on the plasma treated surface and also their perimeter length was statistically longer suggesting cell spreading. Conversely, the roundness of cells on the 20:1 plasma treated substrate was greater than that of the no treated substrate. Hydrophobicity testing could be done on the PDMS and plasma treated PDMS substrates to see how much the plasma treatment changes the hydrophobicity of all three substrates. It may just be effective for the 5:1 substrate as there is not much of a difference noticed between treated and not treated substrates for the 10:1 substrate.

From a purely cell culture point of view, the plasma treated substrates could be used as a cell culture substrate as the cells can adhere more successfully than they could on non-treated PDMS but for the PDMS substrates to be utilised for fixed and time-lapse imaging of the macrophages, it would not be successful as the adherence is not great enough to endure washing steps involved in microscopy preparation. In order to use the substrates to see how the substrate stiffness can alter the macrophages ability to phagocytose, another method to help the cells adhere to the substrate needs to be employed.

To remove the issue of hydrophobicity, previous studies have coated the surface of the substrates with ECM proteins such as fibronectin, collagen, or laminin[47]. Laminin was chosen as it is found in the foundation of most cells and organs. The above experiment was repeated three times and again the morphology was similar across all three PDMS substrates.

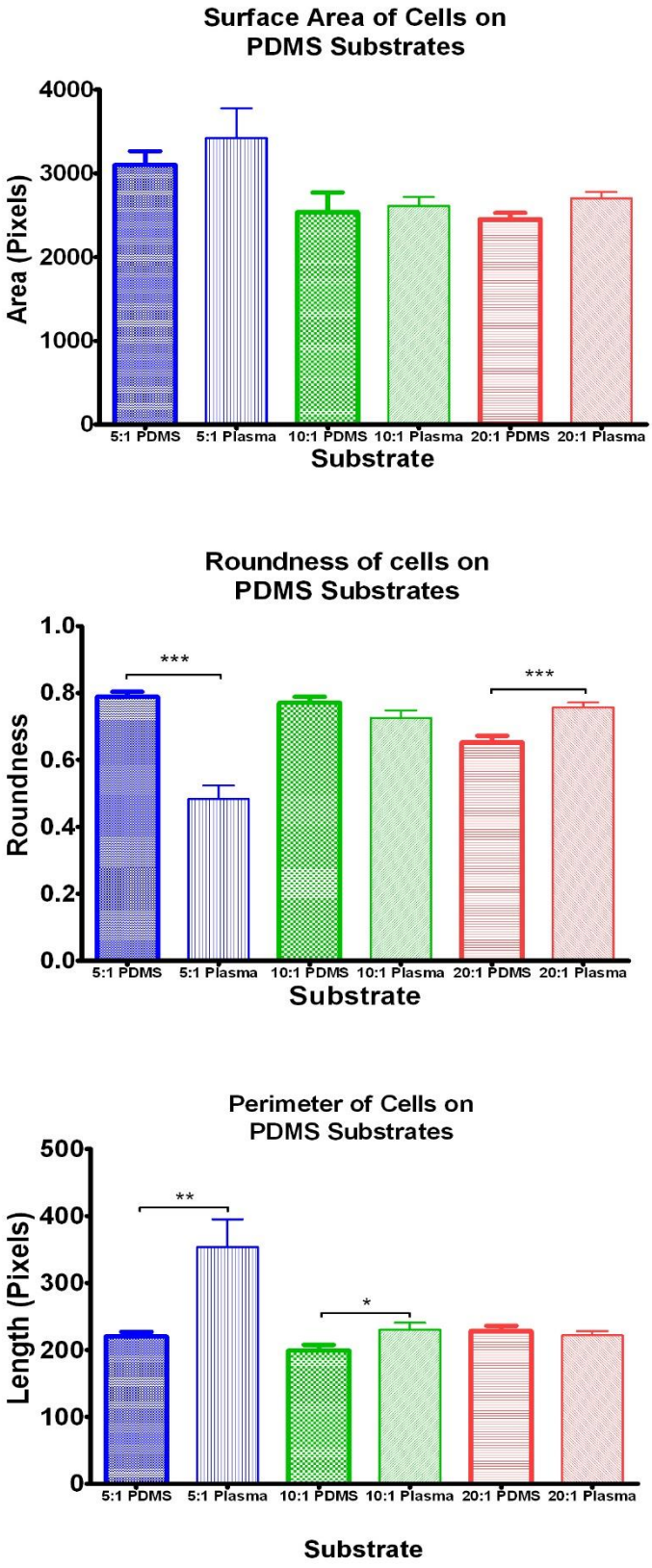

Figure 3.9 A comparison of cells cultured on PDMS and plasma treated PDMS substrates. A. Average surface area of cells was measured and graphed. B. Roundness of cells was calculated and graphed. C Perimeter of cells was measured and graphed for each substrate. Graphs show mean ± SEM (* -> P<0.001, ** -> P<0.01 and *->P<0.05) (N=3).**

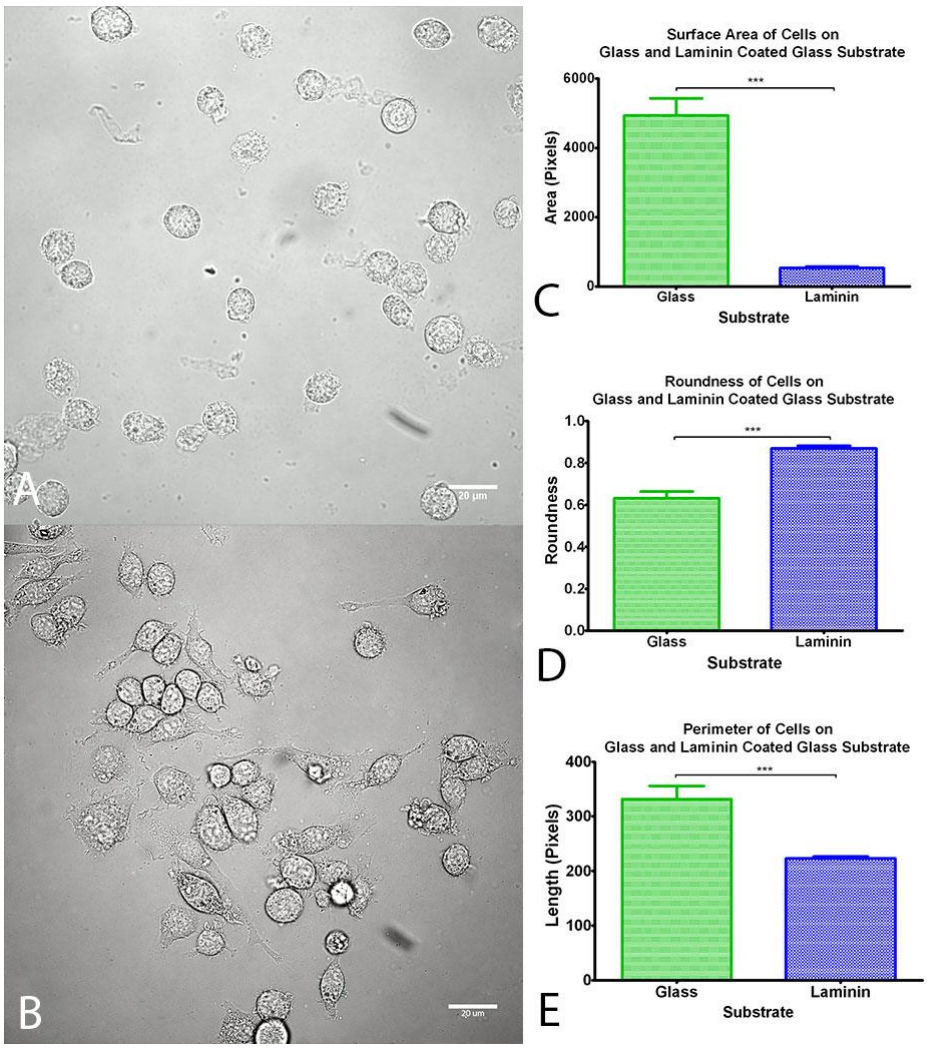

Figure 3.10 Illustrates the morphology of RAW264.7 cells cultured for 48 h on glass (B) and on laminin coated glass (A). C Surface areas of cells was measured and graphed. D Roundness of cells was calculated and graphed for each substrate. E Perimeter of cells was measured and graphed. Graphs show mean ± SEM (* -> P<0.001, ** -> P<0.01 and *->P<0.05) Scale bar shown is 20 µm (N=3).**

The effect of laminin on the morphology of the cells can be clearly seen in Figure 3.10. The laminin caused more cells to adhere than on PDMS substrates alone but they remained very spherical in shape with no cell spreading noticed. In comparison, cells seeded directing onto glass have a very different morphology where they are stretching and reaching with pseudopodia. The surface area and perimeter length of the cells was statistically much greater in cells on the glass substrate. The average roundness of the cells statistically differed between substrates also, with the cells on laminin being much more circular in shape.

Previous studies have used ECM proteins on their substrates but this seems to alter the stiffness of the substrate as seen by the cells[47]. The stiffness testing that had been done on these substrates had been by tensile tests where they stretched the substrates in order to calculate the stiffness. This method seems to ignore the effect the topical ECM proteins may have on the substrate stiffness. In order to see if coating the substrate with an ECM protein had an effect on the stiffness, the substrates were coated with 1 ml of 50 µg/ml of Laminin and the elastic modulus of the substrate was measured using AFM. Substrates were prepared and measured taking at least 30 measurements at different locations on the substrate for each sample. This experiment was repeated on three separate days. The AFM probe indented approximately 200-250 nm on laminin coated substrates, and only approx. 20 nm on PDMS only substrates. The results showed that the stiffnesses of the substrates was drastically altered by the addition of the ECM protein. Coating the PDMS substrates with laminin reduced the elastic modulus for, 5:1 from 42 MPa to 345 kPa, 10:1 from 76 MPa to 1.4 MPa and for the 20:1 from 58 MPa to 320 kPa as seen in figure 3.11 The difference in elastic modulus was statistically significant for all three substrate ratios compared to the laminin coated substrates with $P<0.0001$. A glass cover slip was also coated with laminin and its elastic modulus was measured. This reduced the elastic modulus of glass from the gigapascal range to 441 kPa. The results for the plasma treated PDMS substrates fall in the range of values as previously measured by Mills *et al.*[48].

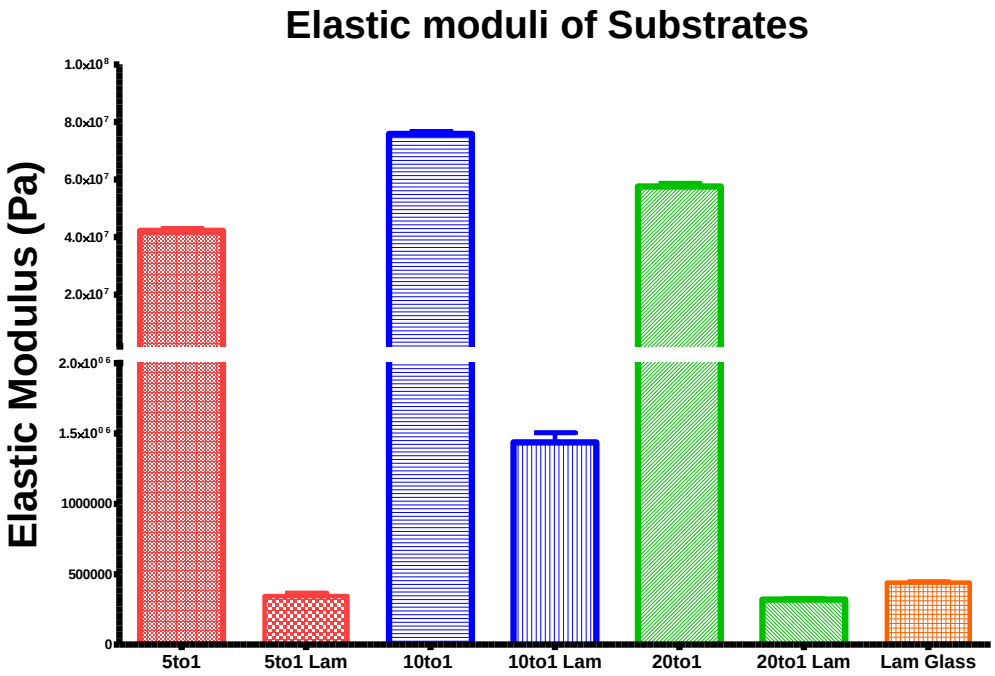

Figure 3.11 Atomic Force Microscopy was used to measure the elastic modulus of the PDMS substrates and also of laminin coated PDMS substrates. The results suggest that the laminin coating adds a "cushion" effect which negates the underneath substrate's stiffness, defeating the purpose of the proposed experiment. Graph shows mean ± SEM (* -> P<0.001, ** -> P<0.01 and *->P<0.05) (N=3).**

There is a variance between the elastic modulus of 10:1 laminin coated substrate in comparison to the other three laminin coated substrates. Although the difference is not statistically significant, a frequency distribution of the 10:1 laminin data was analysed as seen in figure 3.12 and revealed that there was a broad range of values which would suggest that the substrate may not have been uniformly coated with the laminin and thus has a greater mean than the other substrates.

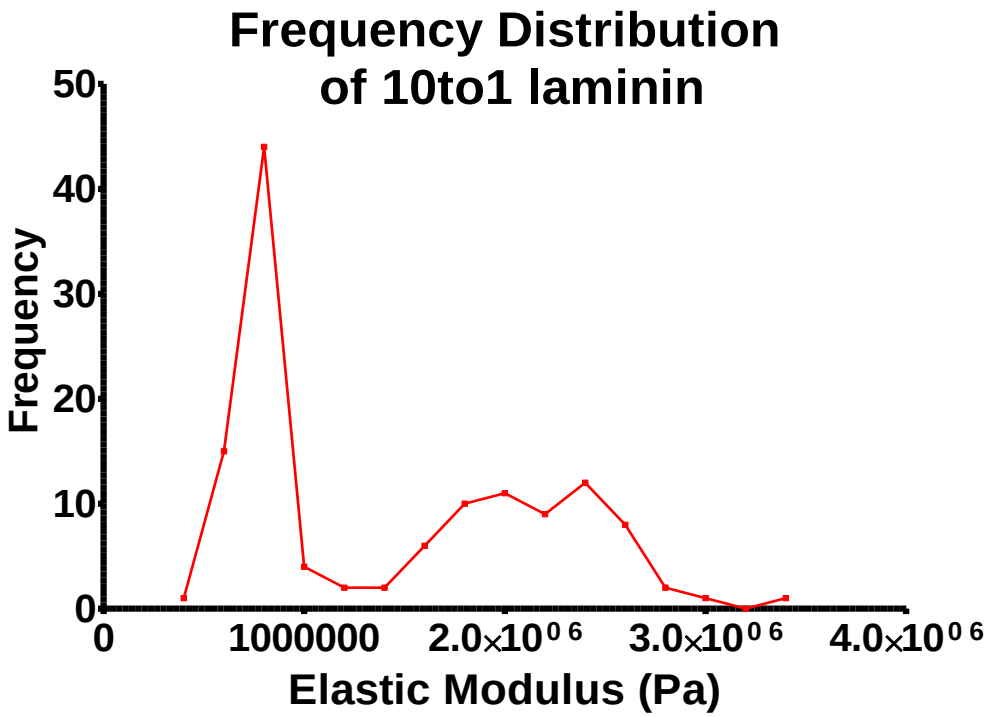

Figure 3.12 Frequency distribution of the 10:1 Laminin coated PDMS substrates showing a range of values suggesting a non-uniform coating of laminin (N=3).

The AFM results clearly demonstrated that coating the substrate with laminin completely alters the stiffness of the substrate and for this reason it should not be used for substrate stiffness experiments. Table 3.33 shows that there is statistical difference between the substrate stiffness pre-laminin coating but after coating the substrates there is no significant difference between the different substrates. Interestingly there is no significant difference between the laminin coated substrates and a laminin coated glass cover slip which suggests that the laminin creates a topical layer on the substrates and the underlying substrate has little to do with stiffness on a nanometre level. The AFM probe indented the substrate by approximatively 200-250 nm on the laminin coated substrates, but only by approximately 20 nm on the plasma treated only samples suggesting a greater stiffness in the non-coated samples as expected.

Bonferroni's Multiple Comparison Test	Significant? P < 0.05?	Summary
5:1 vs 10:1	Yes	***
5:1 vs 20:1	Yes	***
10:1 vs 20:1	Yes	***
5:1 vs 5:1 Laminin	Yes	***
10:1 vs 10:1 Laminin	Yes	***
20:1 vs 20:1 Laminin	Yes	***
5:1 Laminin vs 10:1 Laminin	No	ns
5:1 Laminin vs 20:1 Laminin	No	ns
10:1 Laminin vs 20:1 Laminin	No	ns
5:1 Laminin vs Glass Laminin	No	ns
10:1 Laminin vs Glass Laminin	No	ns
20:1 Laminin vs Glass Laminin	No	ns

Table 3.3 Table of AFM data using a Bonferroni post-hoc test.

3.5 Phagocytic Vesicles

From the time-lapse images of the phagocytosis assay, the phagocytic process ensues as expected from literature except for one extra part that has been noted. After the cup has formed and the pseudopodia have engulfed the bead, it is taken into the cytoplasm where it has now become a phagosome. In some of the cells, there is a premade vesicle that is moved up to where the cup has formed, and the bead is forced into this vesicle to form a phagosome. Figure 3.13 shows this snapshot taken from a time-lapse.

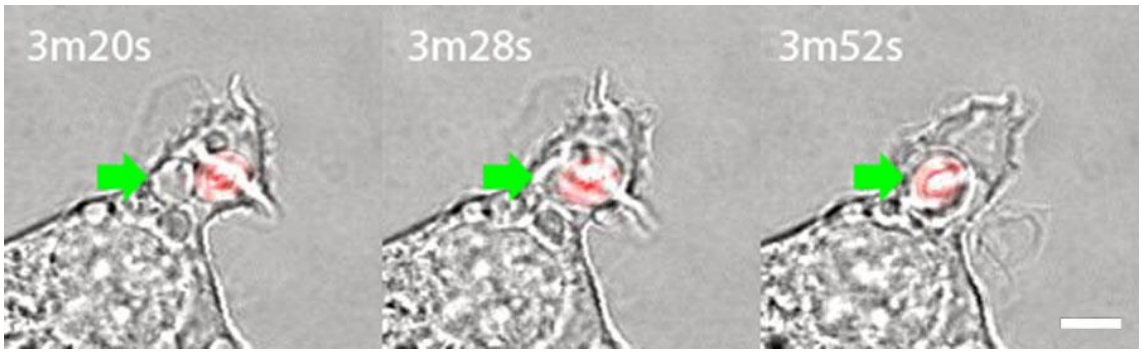

Figure 3.13 RAW264.7 cells showing phagocytosed cy3 tagged zymosan. These stills are taken from a time-lapse to show the phagosome vesicle fusion process. The vesicle is pointed out with the green arrows. Scale bar shown is 10 µm.

The traditional model for phagocytosis states that the membrane bound vesicle or phagosome is formed from the cell membrane when it is pinched on engulfment of the particle into the cytoplasm. In the image at 3m20s it is hard to see any membrane surrounding the bead. After the fusion of the bead and the premade vesicle at 3m28sec it is clear to see the bead has been engulfed by the vesicle. This is clearly seen in the final image which looks like the traditionally expected phagosome.

The phagocytic model says that lysosomes fuse with the phagosome to form a phagolysosome this is expected to be later in the process and not just as the bead is phagocytosed. The vesicle seemed too big to be a lysosome but *lysotracker* was used to confirm if it could possibly be a lysosome. Figure 3.14 shows the cells incubated with *lysotracker* showing the lysosomes in the cell. The vesicles of interest do not fluoresce suggesting they are not lysosomes. Further investigation will need to be done on these vesicles to see exactly what they are.

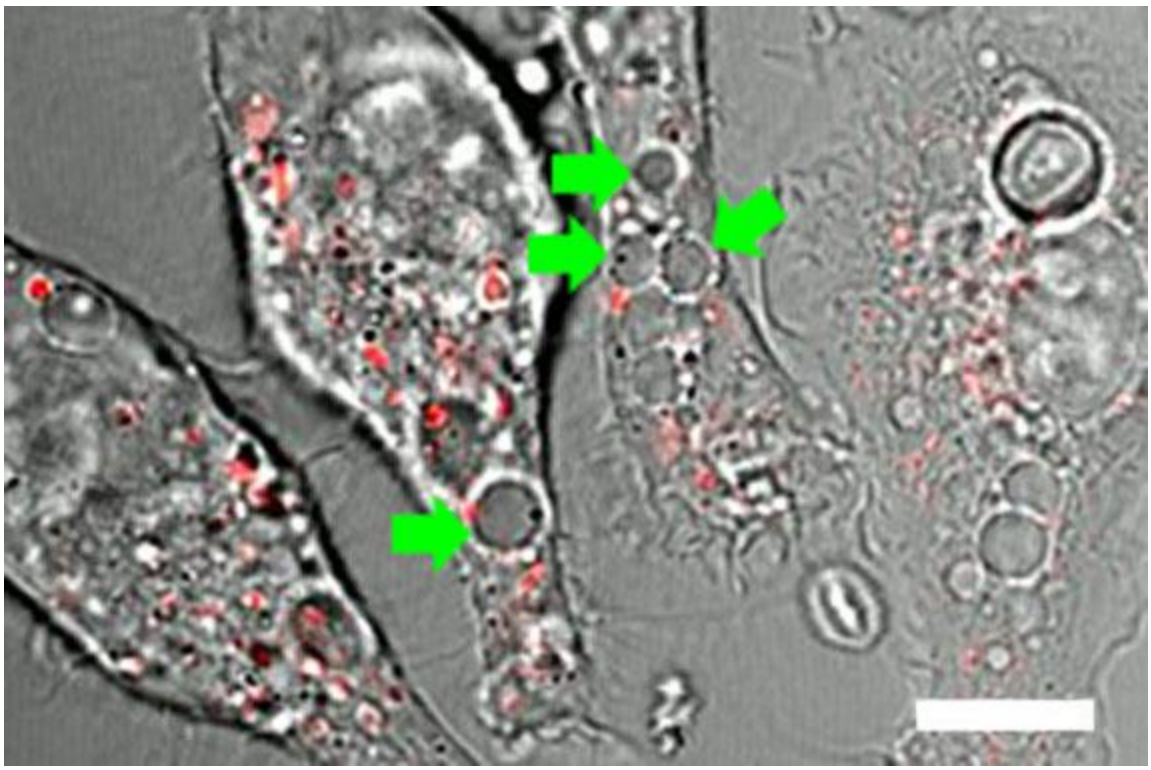

Figure 3.14 RAW264.7 cells showing Lysotracker in red to show lysosomes in the cells. The vesicles are pointed out with the green arrows and show no fluorescence suggesting they are not lysosomes. Scale bar shown is 10 µm.

Chapter 4 - Conclusion

The above studies on the substrate experiments demonstrate that coating the PDMS substrates with laminin negates the stiffness of the substrate underneath. This would suggest that any stiffness studies being carried out would need to be done without using an extracellular matrix such as laminin, collagen or any other which adds an extra layer on the substrates. Another option also needs to be employed to overcome the hydrophobicity of the substrate. The oxygen plasma treatment seemed to be a promising method but due to the nature of PDMS and its plasma treatment recovery, this is not a valid option due to too much variability in the substrates. Taking all this into account, it seems like PDMS is not a suitable substrate for stiffness experiments especially when used for mammalian cell culture work. A different substrate type will have to be chosen and recent studies have shown that hyaluronic acid may be a good substrate.

It is possible to see that both the antibody staining, and the super-resolution imaging have been optimised and are ready for use on the substrates once suitable substrates are chosen. The phagocytic assay has been optimised very successfully for both fixed and time-lapse imaging and the use of SIM super-resolution microscopy has shown good resolution of the proteins of interest which will allow the phagocytic cup formation to be imaged in great detail. As well as that, the time-lapse imaging has revealed that a premade vesicle in the cytoplasm is responsible for the phagosome in some macrophages. This differs from the classical mechanism of phagocytosis and was an unexpected discovery.

Chapter 5 - Future Studies

During my time conducting the above research, many areas of interest for possible other studies presented themselves. If I were to continue with the studies, these are the areas I would like to consider further;

5.1 Substrate Stiffness

Due to the variability of PDMS an alternative suitable substrate would need to be utilised to study the effect of substrate stiffness on macrophages, the stiffnesses can be measured using AFM as above and the surfaces could be compared using electron microscopy to see if surface porosities differ which may have an effect on cell adherence. The hydrophobicity of the substrates would need to be measured by contact angle measurements as this also may have an effect on cell interactions with the substrate as was seen by the difference in hydrophobicity of the PDMS substrates of different ratios.

RAW264.7 and BMDM cells could then be cultured on these substrates and on glass where they would be treated with LPS Bioparticles and Zymosan to see if substrate stiffness has an effect on the macrophages' ability to phagocytose. The above time-lapse imaging could be repeated for each of the substrates to see how stiffness affects the rate of phagocytosis, pseudopodia migration as well as macrophage motility.

As antibodies have already been optimised for the RAW264.7 cell line, it would be possible to stain the cells on the new substrates and see if the expression of vinculin, paxillin, RhoG and talin differ across the different stiffness substrates utilising confocal and SIM super-resolution microscopy. To finish out the substrate work, ELISAs could be performed on the cultured cells to see if the substrate stiffness has an effect on the macrophage activation state as it may cause them to become M1 type activated or more M2 type activated.

These results could suggest that the different stiffness ECMs encountered by macrophages *in vivo* such as scar and cancerous tumour tissues can influence macrophages' ability to phagocytose and also their activation state.

5.2 Phagocytosis Study

Phagocytosis could also be looked at in more detail using super-resolution microscopy on both the N-SIM and STORM Nikon systems. Using these instruments, it would be possible to see the proteins involved in phagocytosis, particularly, the phagocytic cup formation in more detail and higher resolution than has previously been achievable using traditional microscopy techniques.

Myosin isoforms are known to be involved in phagosome internalisation and are very important for the movement of vesicles and other particles along actin fibres which are imperative for phagocytosis. The Rho GTPase family have also been recognised to be important for cytoskeleton remodelling during the phagocytosis process. With this in mind, the RAW264.7 and THP-1 cell lines could be transfected for actin and myosin so time-lapse imaging can be done to see the phagocytosis process in action from cup formation to internalisation. The isolated murine BMDM containing RhoA and Rac1 FRET probes could also allow the investigation of how RhoA and Rac1 are involved in the phagocytosis process as the regulation of actin dynamics is mostly controlled by the Rho GTPase family. It would also be possible to compare fixed samples at various stages of the phagocytic engulfment progression focusing on talin, paxillin, vinculin and RhoG with super-resolution microscopy in order to elucidate their role in the process.

5.3 Vesicle fusion

As well as that, I would like to look in more detail at the initial large vesicle/endosome fusion with the phagosome as seen in the time-lapse images already captured. As stated above, I have already used lysotracker to see if these vesicles were acidic in nature, but they did not appear to be so. Further research would need to be done to find out exactly what these vesicles are and what their involvement is in the phagocytic process.

Ultimately, the goal would be to use the research gathered on phagocytosis with the intention of applying it to a cancer model and see how cancer cells/tumours can affect the macrophages' ability to phagocytose cancer cells. This would be a very important study as it could allow the possibility of activating the macrophages to attack the cancer or even prevent the cancer from metastasising and forming secondary tumours somewhere else in the body.

References

[1] E. Metchnikoff, *L'immunité dans les maladies infectieuses*. Paris, Masson, 1901.

[2] E. Metchnikoff, *Leçons sur la pathologie comparée de l'inflammation : faites à l'Institut Pasteur en 1891*. Paris : Masson, 1892.

[3] A. Parihar, T. D. Eubank, and A. I. Doseff, 'Monocytes and Macrophages Regulate Immunity through Dynamic Networks of Survival and Cell Death', *J. Innate Immun.*, vol. 2, no. 3, pp. 204–215, Apr. 2010.

[4] 'Macrophage Biology Review | macrophages.com'. [Online]. Available: http://www.macrophages.com/macrophage-review. [Accessed: 26-Apr-2016].

[5] R. van Furth and Z. A. Cohn, 'The Origin and Kinetics of Mononuclear Phagocytes', *J. Exp. Med.*, vol. 128, no. 3, pp. 415–435, Sep. 1968.

[6] R. van Furth, Z. A. Cohn, J. G. Hirsch, J. H. Humphrey, W. G. Spector, and H. L. Langevoort, 'The mononuclear phagocyte system: a new classification of macrophages, monocytes, and their precursor cells', *Bull. World Health Organ.*, vol. 46, no. 6, pp. 845–852, 1972.

[7] D. A. Hume, 'The mononuclear phagocyte system', *Curr. Opin. Immunol.*, vol. 18, no. 1, pp. 49–53, Feb. 2006.

[8] S. Yona *et al.*, 'Fate Mapping Reveals Origins and Dynamics of Monocytes and Tissue Macrophages under Homeostasis', *Immunity*, vol. 38, no. 1, pp. 79–91, Jan. 2013.

[9] M. Guilliams *et al.*, 'Alveolar macrophages develop from fetal monocytes that differentiate into long-lived cells in the first week of life via GM-CSF', *J. Exp. Med.*, vol. 210, no. 10, pp. 1977–1992, Sep. 2013.

[10] N. Wang, H. Liang, and K. Zen, 'Molecular Mechanisms That Influence the Macrophage M1–M2 Polarization Balance', *Front. Immunol.*, vol. 5, Nov. 2014.

[11] S. Gordon and F. O. Martinez, 'Alternative Activation of Macrophages: Mechanism and Functions', *Immunity*, vol. 32, no. 5, pp. 593–604, May 2010.

[12] R. E. Vatner, B. T. Cooper, C. Vanpouille-Box, S. Demaria, and S. C. Formenti, 'Combinations of Immunotherapy and Radiation in Cancer Therapy', *Front. Oncol.*, vol. 4, Nov. 2014.

[13] C. C. Bain and A. M. Mowat, 'Macrophages in intestinal homeostasis and inflammation', *Immunol. Rev.*, vol. 260, no. 1, pp. 102–117, Jul. 2014.

[14] A. Tarique, 'Phenotypic, Functional and Plasticity Features of Classical and Alternatively Activated Human Macrophages.', *Am. J. Respir. Cell Mol. Biol.*, 2015.

[15] P. R. Taylor, L. Martinez-Pomares, M. Stacey, H.-H. Lin, G. D. Brown, and S. Gordon, 'Macrophage Receptors and Immune Recognition', *Annu. Rev. Immunol.*, vol. 23, no. 1, pp. 901–944, 2005.

[16] F. O. Martinez, A. Sica, A. Mantovani, and M. Locati, 'Macrophage activation and polarization', *Front. Biosci. J. Virtual Libr.*, vol. 13, pp. 453–461, 2008.

[17] C. D. Mills, 'Macrophage arginine metabolism to ornithine/urea or nitric oxide/citrulline: a life or death issue', *Crit. Rev. Immunol.*, vol. 21, no. 5, pp. 399–425, 2001.

[18] S. M. Morris, 'Recent advances in arginine metabolism: roles and regulation of the arginases', *Br. J. Pharmacol.*, vol. 157, no. 6, pp. 922–930, Jul. 2009.

[19] K. J. Mylonas, M. G. Nair, L. Prieto-Lafuente, D. Paape, and J. E. Allen, 'Alternatively Activated Macrophages Elicited by Helminth Infection Can Be Reprogrammed to Enable Microbial Killing', *J. Immunol.*, vol. 182, no. 5, pp. 3084–3094, Mar. 2009.

[20] P. J. Murray *et al.*, 'Macrophage Activation and Polarization: Nomenclature and Experimental Guidelines', *Immunity*, vol. 41, no. 1, pp. 14–20, Jul. 2014.

[21] J. G. Quatromoni and E. Eruslanov, ‘Tumor-associated macrophages: function, phenotype, and link to prognosis in human lung cancer’, *Am. J. Transl. Res.*, vol. 4, no. 4, pp. 376–389, Oct. 2012.
[22] B.-Z. Qian and J. W. Pollard, ‘Macrophage Diversity Enhances Tumor Progression and Metastasis’, *Cell*, vol. 141, no. 1, pp. 39–51, Apr. 2010.
[23] C. Alexander and E. T. Rietschel, ‘Invited review: Bacterial lipopolysaccharides and innate immunity’, *J. Endotoxin Res.*, vol. 7, no. 3, pp. 167–202, Jun. 2001.
[24] R. Jerala, ‘Structural biology of the LPS recognition’, *Int. J. Med. Microbiol.*, vol. 297, no. 5, pp. 353–363, Sep. 2007.
[25] D. M. Underhill *et al.*, ‘The Toll-like receptor 2 is recruited to macrophage phagosomes and discriminates between pathogens’, *Nature*, vol. 401, no. 6755, pp. 811–815, Oct. 1999.
[26] W. L. Murphy, T. C. McDevitt, and A. J. Engler, ‘Materials as stem cell regulators’, *Nat. Mater.*, vol. 13, no. 6, pp. 547–557, Jun. 2014.
[27] K. A. Kilian and M. Mrksich, ‘Directing Stem Cell Fate by Controlling the Affinity and Density of Ligand-Receptor Interactions at the Biomaterials Interface’, *Angew. Chem. Int. Ed.*, vol. 51, no. 20, pp. 4891–4895, May 2012.
[28] A. J. Engler, S. Sen, H. L. Sweeney, and D. E. Discher, ‘Matrix Elasticity Directs Stem Cell Lineage Specification’, *Cell*, vol. 126, no. 4, pp. 677–689, Aug. 2006.
[29] R. Sridharan, A. R. Cameron, D. J. Kelly, C. J. Kearney, and F. J. O’Brien, ‘Biomaterial based modulation of macrophage polarization: a review and suggested design principles’, *Mater. Today*, vol. 18, no. 6, pp. 313–325, Jul. 2015.
[30] A. K. Blakney, M. D. Swartzlander, and S. J. Bryant, ‘The effects of substrate stiffness on the in vitro activation of macrophages and in vivo host response to poly(ethylene glycol)-based hydrogels’, *J. Biomed. Mater. Res. A*, vol. 100, no. 6, pp. 1375–1386, Jun. 2012.
[31] M. L. Previtera and A. Sengupta, ‘Substrate Stiffness Regulates Proinflammatory Mediator Production through TLR4 Activity in Macrophages’, *PLOS ONE*, vol. 10, no. 12, p. e0145813, Dec. 2015.
[32] K. M. Adlerz, H. Aranda-Espinoza, and H. N. Hayenga, ‘Substrate elasticity regulates the behavior of human monocyte-derived macrophages’, *Eur. Biophys. J.*, vol. 45, no. 4, pp. 301–309, Nov. 2015.
[33] S. Mondal *et al.*, ‘PTEN Negatively Regulates Engulfment of Apoptotic Cells by Modulating Activation of Rac GTPase’, *J. Immunol.*, vol. 187, no. 11, pp. 5783–5794, Dec. 2011.
[34] J. S. Kim, X. Peng, P. K. De, R. L. Geahlen, and D. L. Durden, ‘PTEN controls immunoreceptor (immunoreceptor tyrosine-based activation motif) signaling and the activation of Rac’, *Blood*, vol. 99, no. 2, pp. 694–697, Jan. 2002.
[35] A. M. Labrousse *et al.*, ‘Frustrated Phagocytosis on Micro-Patterned Immune Complexes to Characterize Lysosome Movements in Live Macrophages’, *Front. Immunol.*, vol. 2, Oct. 2011.
[36] M. Hagiwara *et al.*, ‘Vinculin and Rab5 Complex Is Requited for Uptake of Staphyrococcus aureus and Interleukin-6 Expression’, *PLoS ONE*, vol. 9, no. 1, p. e87373, Jan. 2014.
[37] M. Gitik, R. Kleinhaus, S. Hadas, F. Reichert, and S. Rotshenker, ‘Phagocytic receptors activate and immune inhibitory receptor SIRPα inhibits phagocytosis through paxillin and cofilin’, *Front. Cell. Neurosci.*, vol. 8, Apr. 2014.
[38] K. Kedzierska, N. J. Vardaxis, A. Jaworowski, and S. M. Crowe, ‘FcγR-mediated phagocytosis by human macrophages involves Hck, Syk, and Pyk2 and is augmented by GM-CSF’, *J. Leukoc. Biol.*, vol. 70, no. 2, pp. 322–328, Aug. 2001.

[39] J. Lim, A. Wiedemann, G. Tzircotis, S. J. Monkley, D. R. Critchley, and E. Caron, 'An Essential Role for Talin during αMβ2-mediated Phagocytosis', *Mol. Biol. Cell*, vol. 18, no. 3, pp. 976–985, Mar. 2007.
[40] 'Colocalization of F-actin and talin during Fc receptor-mediated phagocytosis in mouse macrophages', *J. Exp. Med.*, vol. 172, no. 6, pp. 1853–1856, Dec. 1990.
[41] D. Li *et al.*, 'Extended-resolution structured illumination imaging of endocytic and cytoskeletal dynamics', *Science*, vol. 349, no. 6251, p. aab3500, Aug. 2015.
[42] T. A. Klar and S. W. Hell, 'Subdiffraction resolution in far-field fluorescence microscopy', *Opt. Lett.*, vol. 24, no. 14, pp. 954–956, Jul. 1999.
[43] D. Wildanger *et al.*, 'Solid Immersion Facilitates Fluorescence Microscopy with Nanometer Resolution and Sub-Ångström Emitter Localization', *Adv. Mater.*, vol. 24, no. 44, pp. OP309-OP313, Nov. 2012.
[44] B. Huang, W. Wang, M. Bates, and X. Zhuang, 'Three-dimensional Super-resolution Imaging by Stochastic Optical Reconstruction Microscopy', *Science*, vol. 319, no. 5864, pp. 810–813, Feb. 2008.
[45] E. Betzig *et al.*, 'Imaging intracellular fluorescent proteins at nanometer resolution', *Science*, vol. 313, no. 5793, pp. 1642–1645, Sep. 2006.
[46] N. Olivier, D. Keller, P. Gönczy, and S. Manley, 'Resolution Doubling in 3D-STORM Imaging through Improved Buffers', *PLOS ONE*, vol. 8, no. 7, p. e69004, Jul. 2013.
[47] L. Wang, B. Sun, K. S. Ziemer, G. A. Barabino, and R. L. Carrier, 'Chemical and physical modifications to poly(dimethylsiloxane) surfaces affect adhesion of Caco-2 cells', *J. Biomed. Mater. Res. A*, vol. 93A, no. 4, pp. 1260–1271, Jun. 2010.
[48] K. L. Mills, X. Zhu, S. Takayama, and M. D. Thouless, 'The mechanical properties of a surface-modified layer on poly(dimethylsiloxane)', *J. Mater. Res.*, vol. 23, no. 1, pp. 37–48, Jan. 2008.
[49] D. Bodas and C. Khan-Malek, 'Hydrophilization and hydrophobic recovery of PDMS by oxygen plasma and chemical treatment—An SEM investigation', *Sens. Actuators B Chem.*, vol. 123, no. 1, pp. 368–373, Apr. 2007.